Immunofluorescence analysis. Tissues were processed as for immunohistochemistry, with the exception that sections were not exposed to hydrogen peroxide. Sections were incubated for 40 min at room temperature with 10 mM HCl containing pepsin, and incubated for 60 min at room temperature with 2 N HCl then 0.1 M sodium tetraborade (pH 8.5), washed three times with PBS before exposure for 1 h at 30°C to primary antibodies diluted in PBS. The sections were washed three times with PBS, incubated with appropriate Alexa Fluor 488-conjugated or Texas red-conjugated secondary antibody (Invitrogen, Tokyo, Japan), diluted in PBS, washed three times with PBS, and mounted in Vectashield mounting medium (Vector Laboratories). Sections were viewed and photographed with a Biorevo BZ-9000 fluorescence microscope (Keyence, Tokyo, Japan).

Antibodies. The IM7 (diluted 1:100) and CD44v8-10 (1:100) antibodies were used to detect mouse CD44 and CD44 variant (CD44v), respectively. Proliferating cells were detected with the Ki67 antibody (clone Bu201, 1:50; DakoCytomation).

Preparation of rat monoclonal antibody recognizing mouse CD44v. Female F344 rats were repeatedly immunized with RH7777 cells expressing mouse CD44v8-10-GFP. Three days after the final immunization, rat spleen cells were fused to X63 mouse myeloma cells with PEG (Roche Diagnostics, Tokyo, Japan). Selected and established hybridoma clones were inoculated to KSN athymic mice pretreated with tetramethylpentadecane (pristane). Ascitic fluids were precipitated with 50%-saturated ammonium sulfate. Further purification was done by affinity chromatography with protein G-conjugated Sepharose (GE Healthcare, Uppsala, Sweden).

Cell preparation and FACS analysis. Mouse gastric tumors from 30-week-old *K19-Wnt1/C2mE* mice were digested for 3 h at 37°C in Ham's F12 medium with 5% FCS, 100 U/mL penicillin, 100 μg/mL streptomycin, 5 μg/mL insulin, 300 U/mL collagenase, and 100 U/mL hyaluronidase. This digested solution was vortexed, then the red blood cells were lysed in NH_4Cl at room temperature. A single cell suspension was obtained by sequential dissociation of the fragments by gentle pipetting in 0.25% trypsin (1–2 min) and 5 mg/mL dispase with 0.1 mg/mL DNase I (2 min). The solution was then filtered through a 40-μm nylon mesh. All reagents were purchased from Stemcell Technologies (Vancouver, Canada).

Single suspended cells were incubated with antibodies at 4°C for 30 min. Antibodies for FACS analysis, CD31-FITC, CD45-FITC, TER119-FITC, CD44-APC, and CD133-PE were purchased from eBioscience (San Diego, CA, USA). Dissociated Lin^- ($CD45^-$, $TER119^-$, $CD31^-$), propidium $iodide^-$ (non-apoptotic) gastric tumor cells were sorted by FACSAria Cell Sorter (BD Biosciences, Tokyo, Japan) using anti-CD44 antibody.

Quantitative and semiquantitative RT-PCR analysis. Total RNA was extracted from the sorted tumor cells using Isogen (Nippon Gene, Tokyo, Japan), and was subjected to RT-PCR with specific primers, and those specific for GAPDH were used as an internal control. Primers for detection of CD44v mRNAs were targeted to exons 5 and 16, as described previously.[11] Quantitative RT-PCR was carried out using the Thermal Cycler Dice Real Time System (Takara Bio, Tokyo, Japan). The PCR conditions were as follows: 95°C for 2 min, and 40 cycles at 95°C for 30 s, 60°C for 30 s, followed by dissociation-curve analysis to confirm specificity. Data are presented as means ± SD of triplicates. Primer sets for RT-PCR were: CD44v forward, 5′-GGAGATCAGGATGACTCCTTCT-3′ and reverse, 5′-AGTCCTTGGATGAGTCTCGATC-3′; MUC5AC forward, 5′-CTACCACTCCCTGCTTCTGC-3′ and reverse, 5′-TCCTGGCTACACATCGCATA-3′; CD133 forward, 5′-GAAAAGTTGCTCTGCGAACC-3′ and reverse, 5′-CTCGACCTCTTTTGCAATCC-3′; and GAPDH forward, 5′-GTGAAGGTCGGTGTGAACG-3′ and reverse, 5′-GACCATGTAGTTGAGGTCAATG-3′.

Statistical analysis. Data are presented as means ± SD and were analyzed using the unpaired Student's *t*-test in Excel 2007 (Microsoft, Redmond, WA, USA). A value of $P < 0.05$ was considered statistically significant.

Results

CD44 differentially expressed in undifferentiated cells located at center of gastric tumors in *K19-Wnt1/C2mE* mice. *K19-Wnt1/C2mE* mouse, which overexpress Wnt1, COX2 and microsomal prostaglandin E synthase 1 (mPGES-1) in gastric epithelial cells, is a genetic model for gastric carcinogenesis.[9] Simultaneous activation of both Wnt and PGE_2 pathways causes large dysplastic gastric tumors, and all of these transgenic animals became moribund at approximately 30–50 weeks of age. One hundred percent of the gastric tumors in *K19-Wnt1/C2mE* mice arose from the region of the SCJ (Fig. 1A–C).[9] Although keratin 19 promoter is active in pancreas and intestines as well as stomach, we did not find any tumor formation in the tissues other than stomach because the expression of transgenes, *COX2* and *mPGES-1*, was silenced in those tissues by an unknown mechanisms, as we previously described.[12]

We first examined the expression and distribution of the CSC marker CD44 in gastric tumors of 30-week-old *K19-Wnt1/C2mE* mice (Fig. 1D). Immunohistochemical analysis revealed that CD44 expression is predominantly present in the center of the gastric tumors (Fig. 1E) and weakly present toward the periphery of the tumor (Fig. 1F). These results indicate that the majority of $CD44^+$ tumor cells are preferentially located in the central regions of gastric tumors. Given that the increased expression of CD44 splicing variant isoforms (CD44v) is associated with tumor progression in various human adenocarcinomas,[13,14] we next investigated CD44v expression in tumors of *K19-Wnt1/C2mE* mice. Using RT-PCR analysis we detected the expression of three variant isoforms in addition to the standard form, and the DNA sequence analysis revealed that those variant isoforms included exons v6-10, v7-10, and v8-10 (Fig. 1G). To further investigate the expression of CD44v in *K19-Wnt1/C2mE* mice, we generated an antibody against the mouse CD44 v8-10 epitope and found that CD44v is expressed predominantly in tumor cells of *K19-Wnt1/C2mE* mice (Fig. 1H).These results are consistent with previous observations in human gastric adenocarcinoma.[14,15]

To characterize $CD44^+$ tumor cells, we isolated $CD44^+$ or $CD44^-$ tumor cells from gastric tumors of *K19-Wnt1/C2mE* mice by FACS and examined the mRNA expression of CD133, a potential marker of undifferentiated cells in the gastrointestinal tract,[16] and the gastric epithelial differentiation marker MUC5AC.[17] $CD44^+$ tumor cells show a high level of CD133 expression (Fig. 1I) and a low level of MUC5AC expression compared to $CD44^-$ cells (Fig. 1J). Furthermore, FACS analysis revealed that a large population of $CD44^+$ cells (42.7%) express high levels of CD133 compared to $CD44^-$ cells (Fig. 1K). Based on these findings, we assumed that CD44, which is expressed in undifferentiated gastric tumor cells that are located in the center of the tumor, plays a role in the maintenance and development of gastric tumors.

$CD44^+$ gland at SCJ region of normal mouse stomach contains some slow-cycling cells. The SCJ region corresponds to the esophagus–columnar junction (EC junction) in humans and is a frequent site of tumor development.[18,19] Therefore, we speculated that the normal SCJ region would contain cells that are susceptible to gastric carcinogenesis. In the corpus of the normal mouse stomach, $CD44^+$ gastric epithelial cells were rarely detected. However, we found one gland in the vicinity of the SCJ that contains cells expressing high levels of CD44 (Fig. 2A). $CD44^+$ cells tended to be localized along the basal side of the gland. We then immunohistochemically investigated

doi: 10.1111/j.1349-7006.2009.01430.x

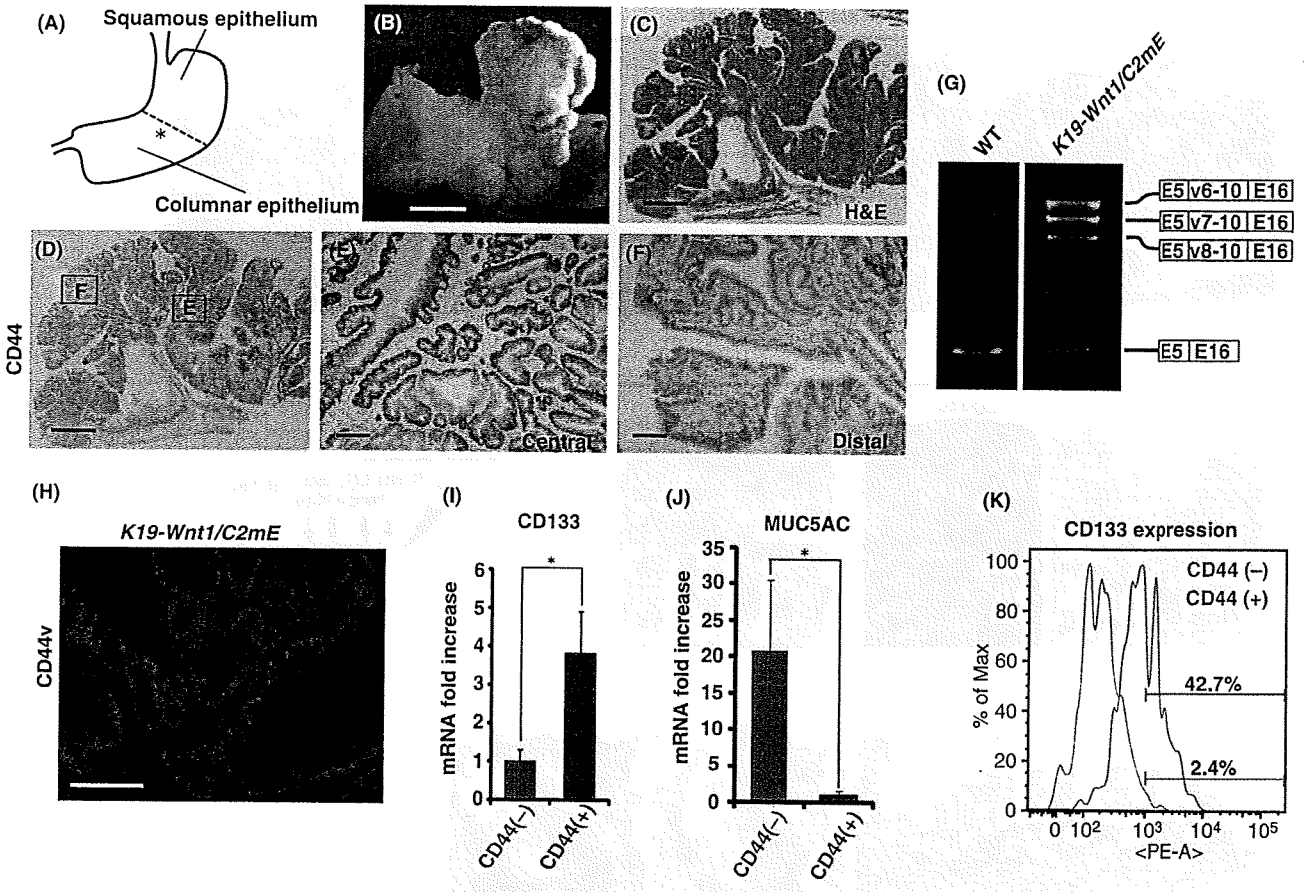

Fig. 1. Pattern of CD44 expression in gastric tumors of *K19-Wnt1/C2mE* mice. (A–C) Left panel shows a diagram of the wild-type mouse stomach (A). The asterisk indicates the squamo-columnar junction region. Macroscopic image (B) and H&E staining (C) of the stomach from a 30-week-old *K19-Wnt1/C2mE* mouse. (D–F) Immunohistochemical staining for CD44 (D) in the stomach of a 30-week-old *K19-Wnt1/C2mE* mouse. The central (E) and distal (F) region of the gastric tumor is shown at higher magnification in the middle and right panels, respectively. Scale lines = 5 mm (B), 1 mm (C,D), and 100 μm (E,F). (G) Total RNA isolated from gastric mucosa of 30-week-old wild-type and gastric tumors of 30-week-old *K19-Wnt1/C2mE* mice, was subjected to RT-PCR analysis with specific primers targeted to exon 5 and 16 of CD44 mRNA. Direct sequencing of the PCR products revealed that CD44 variant (CD44v) (v6-10, v7-10, v8-10) was predominantly expressed in the gastric tumors of *K19-Wnt1/C2mE* mice. (H) Immunofluorescence analysis of CD44v in gastric tumors of 30-week-old *K19-Wnt1/C2mE* mice. Scale line = 100 μm. (I) Expression of CD133 in $CD44^+$ cells relative to that in $CD44^-$ cells. Lin^- ($CD45^-$, $TER119^-$, $CD31^-$), propidium $iodide^-$ (non-apoptotic) gastric tumor cells were separated by FACS using anti-CD44 antibody and subjected to quantitative RT-PCR analysis. $^*P < 0.01$. (J) Expression of MUC5AC in $CD44^-$ cells relative to that in $CD44^+$ cells were determined by quantitative RT-PCR analysis using a similar method to that outlined in (G). $^*P < 0.01$. (K) Flow cytometric analysis of CD133 expression in $CD44^+$ or $CD44^-$ cells. A control was included in the negative fraction ($0–10^3$).

whether these $CD44^+$ cells express the standard form or variant isoform of CD44. We found that $CD44^+$ cells located at SCJ gland express CD44 variant isoform like tumor cells (Fig. 2B). This result suggests that gastric tumor in *K19-Wnt1/C2mE* mice might be a result of neoplastic expansion of $CD44v^+$ cells at the SCJ gland. To further characterize $CD44^+$ cells located in the SCJ gland, we examined the proliferation status in these cells. Such $CD44^+$ cells in the SCJ gland were mostly negative for Ki67, a marker of cell proliferation (Fig. 2B), suggesting that they are quiescent or slow-cycling stem-like cells located near proliferative progenitor cells.

We carried out BrdU labeling assays (Fig. 2C) to investigate whether $CD44^+$ gastric cells in the SCJ gland showed a characteristic peculiar to tissue stem cells, that is, slow cycling and retention of the BrdU label in the nucleus over several weeks.[20] Immunohistochemical analysis done by sequentially staining with antibodies against BrdU and CD44 revealed that a few label-retaining cells (LRCs) were located in the base of the SCJ gland and that those LRCs expressed high levels of CD44 (Fig. 2D). These results suggested that these rare $CD44^+$ SCJ cells have stem-like quiescent or slow-cycling characteristics.

PGE_2-mediated signaling is essential for the expansion of $CD44^+$ SCJ gland cells. Given that duplication of gastric glands is thought to be mediated by stem cell division,[21] we hypothesized that $CD44^+$ SCJ cells would be cells-of-origin of the gastric tumors that develop in *K19-Wnt1/C2mE* mice. Our hypothesis was supported by immunohistochemical analysis of the SCJ region in *K19-Wnt1/C2mE* mice at 12, 20, and 30 weeks of age, which showed that the $CD44^+$ gland cells expanded concomitantly with gastric tumor development (Fig. 3A,B).

Wnt/β-catenin signaling is known to promote the proliferation and self-renewal of stem cells or progenitors during the development of a variety of tissues.[22] PGE_2 signaling has also been found to enhance the number of stem cells and multipotent progenitors in the hematopoietic system.[23] Therefore, we next investigated whether the expansion of $CD44^+$ SCJ cells in the transgenic mice is mediated by PGE_2 or Wnt1 signaling. $CD44^+$ SCJ cells were significantly expanded in 40-week-old *K19-C2mE* mice, which overexpress COX2 and mPGES-1 and develop preneoplastic hyperplastic legions. In contrast, $CD44^+$ SCJ cells were not expanded in *K19-Wnt1* mice, which

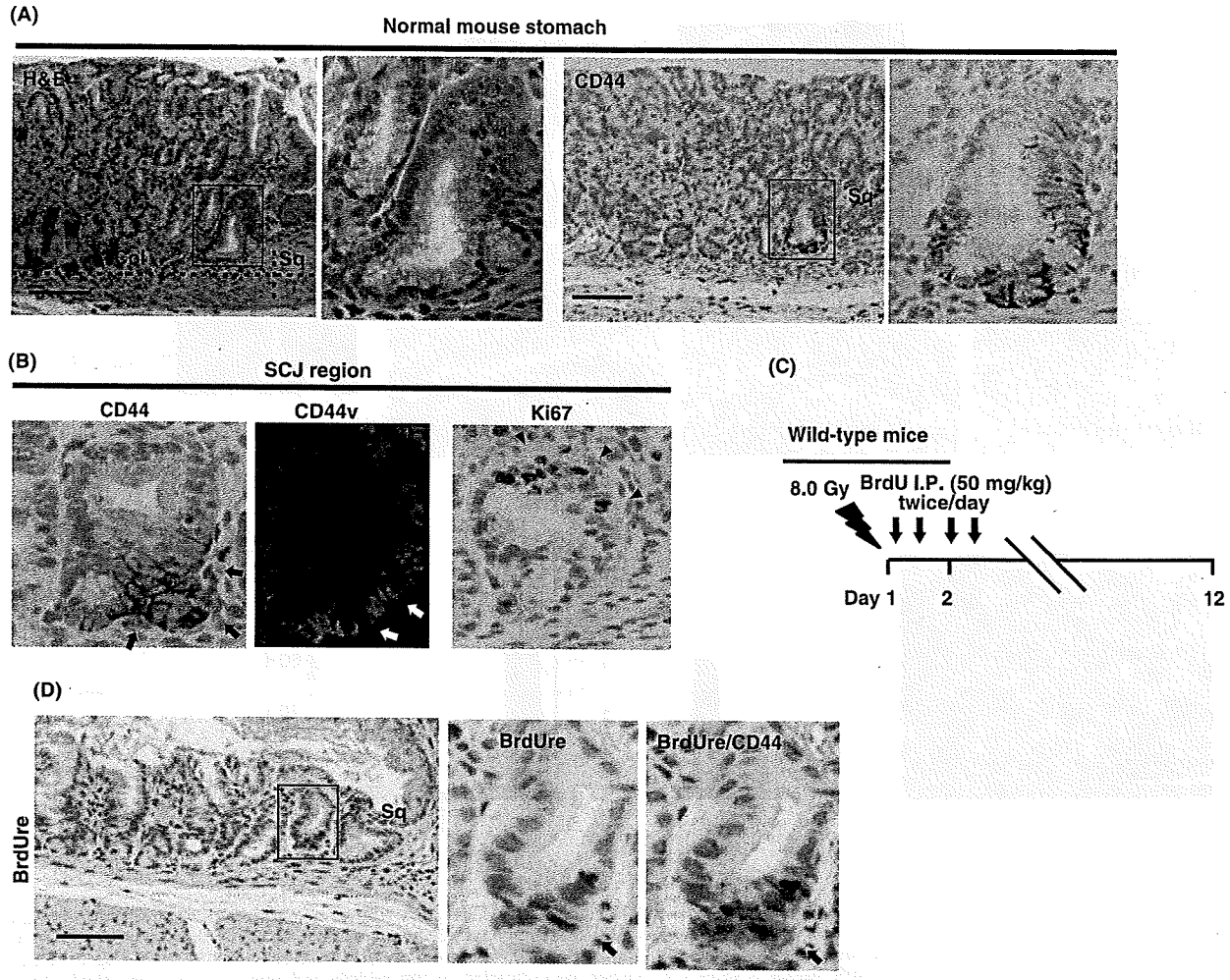

Fig. 2. CD44$^+$ gland cells at the squamo-columnar junction (SCJ) region in mouse stomach include label-retaining cells. (A) H&E staining and immunohistochemical staining for CD44 in the SCJ region in wild-type mouse stomach. The boxed regions in the left panels are shown at higher magnification in the right panels. Col, columnar epithelium; Sq, squamous epithelium. (B) Immunohistochemical staining for CD44 and Ki67 and immunofluorescence analysis of CD44 variant (CD44v) of the SCJ region in wild-type mouse stomach. Black arrows (white arrows) and arrowheads indicate mutually exclusive expression of CD44 (CD44v) and Ki67, respectively. (C) The protocol for the BrdU label-retention assay using wild-type mice. (D) Immunohistochemical staining for BrdU in the SCJ region 10 days after BrdU injection. The boxed region in the left panel is shown at a higher magnification in the middle panel and the right panel shows double staining for BrdU and CD44 in the same section. Arrows indicate BrdU label-retaining cells in the SCJ region. Scale bars = 100 μm.

overexpress Wnt1 (Fig. 3C,D). These data indicate that PGE_2-mediated signaling plays a major role in the expansion of CD44$^+$ SCJ cells. Importantly, Wnt1 expression strongly enhanced the expansion of CD44$^+$ SCJ cells in the presence of PGE_2 signaling (Fig. 3D), leading to gastric tumorigenesis. PGE_2 signaling has been shown to induce cyclic AMP/protein kinase A-mediated phosphorylation of β-catenin, leading to the stabilization of β-catenin and activation of Wnt signaling in hematopoietic stem/progenitor cells.[24] Taken together, these results suggest that the effects of PGE_2 signaling are prominently enhanced by Wnt signaling in CD44$^+$ stem-like cells.

Majority of expanding slow-cycling tumor cells express high levels of CD44. If the increased number of CD44$^+$ gland cells in *K19-Wnt1/C2mE* mice tumors is due to expansion of the SCJ gland, then slow-cycling LRCs might exist among the CD44$^+$ gland cells. To test this hypothesis, we carried out assays to measure long-term BrdU label retention using *K19-Wnt1/C2mE* mice (Fig. 4A). Immunohistochemical analysis revealed that LRCs are mainly detected in CD44$^+$ gland cells located in the central region of tumors, whereas only a few LRCs were found in the CD44$^-$ cells or cells expressing low levels of CD44 in the periphery of the tumors (Fig. 4B,C). These findings suggest that gastric tumors in the transgenic mouse model are initiated by expansion of specific SCJ gland cells consisting of CD44$^+$ quiescent or slow-cycling stem-like cells.

Discussion

In this study, we found that the SCJ region of the normal mouse stomach contains a gland consisting of CD44$^+$ cells, of which a few are quiescent or slow-cycling stem cell-like gastric cells. Furthermore, we showed that this characteristic gland containing the stem-like CD44$^+$ SCJ cells expands in response to PGE_2-mediated signaling and constructs preneoplastic lesions. The cell fate in the SCJ region is determined by conflicting extrinsic signals from the two adjacent epithelial tissues, namely squamous and glandular tissues, and this region of the mouse stomach is thus considered to be highly susceptible to oncogenesis.[25]

doi: 10.1111/j.1349-7006.2009.01430.x

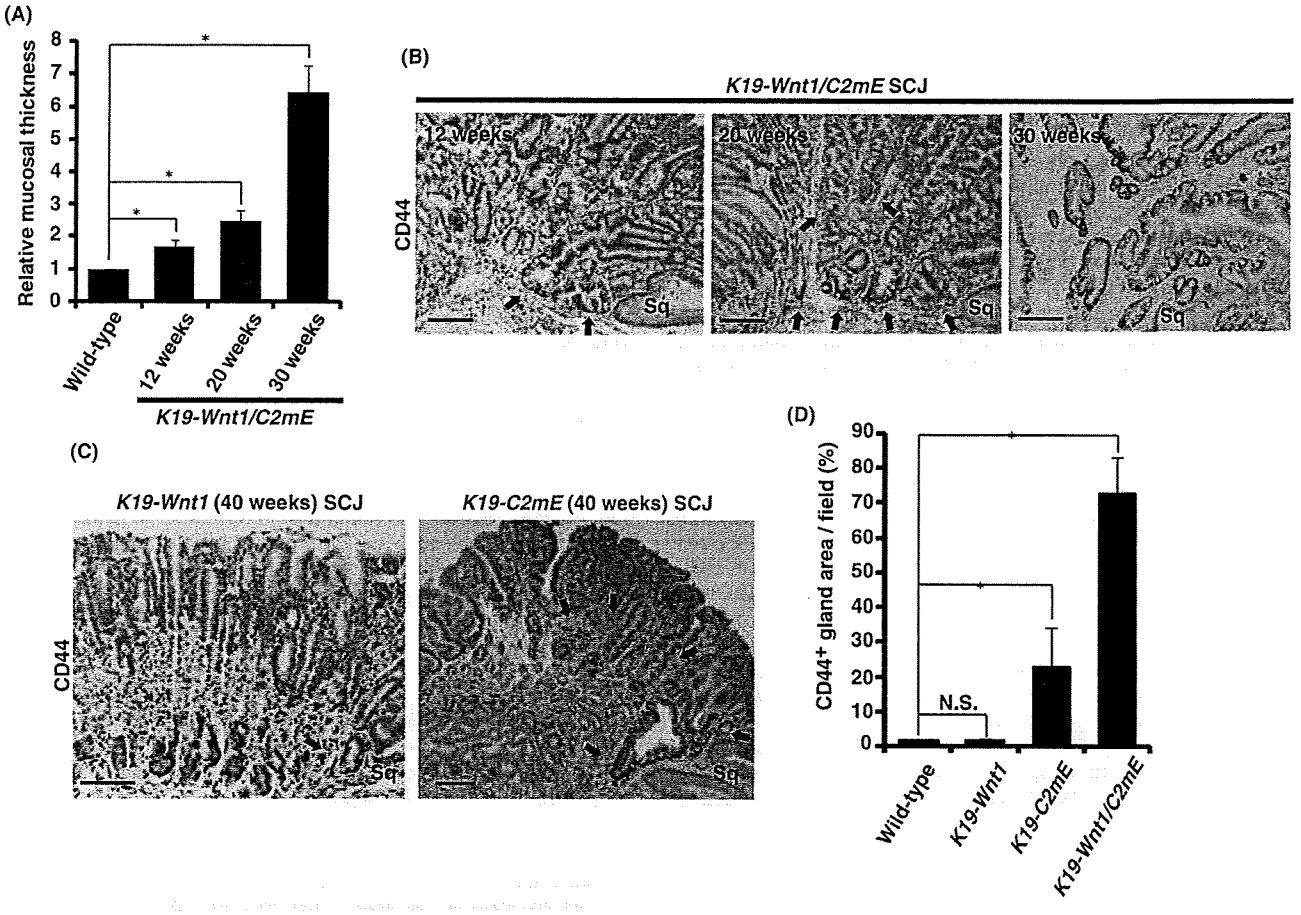

Fig. 3. CD44$^+$ gland cells are expanded in *K19-C2mE* mice but not in *K19-Wnt1* mice. (A) The gastric mucosal thickness, which reflects the size of the tumor, in *K19-Wnt1/C2mE* mice at the indicated ages relative to that in age-matched wild-type mice. Data are means ± SD from three mice. *$P < 0.05$ *versus* wild-type mice. (B) Immunohistochemical staining for CD44 at the squamo-columnar junction (SCJ) region in the stomach of *K19-Wnt1/C2mE* mice at 12, 20, and 30 weeks of age. CD44$^+$ gland cells (arrows) are expanded concomitant with tumor development. Scale bars = 100 μm. (C) Immunohistochemical staining for CD44 at the SCJ region of *K19-Wnt1* or *K19-C2mE* mice at 40 weeks of age. Arrows indicate CD44$^+$ gastric glands at the SCJ region. Scale bars = 100 μm. (D) Percentage of CD44$^+$ gland cell area per field of wild-type, *K19-Wnt1*, and *K19-C2mE* mice at 40 weeks of age, and *K19-Wnt1/C2mE* mice at 30 weeks of age. Data are means ± SD from three mice of each genotype. *$P < 0.01$.

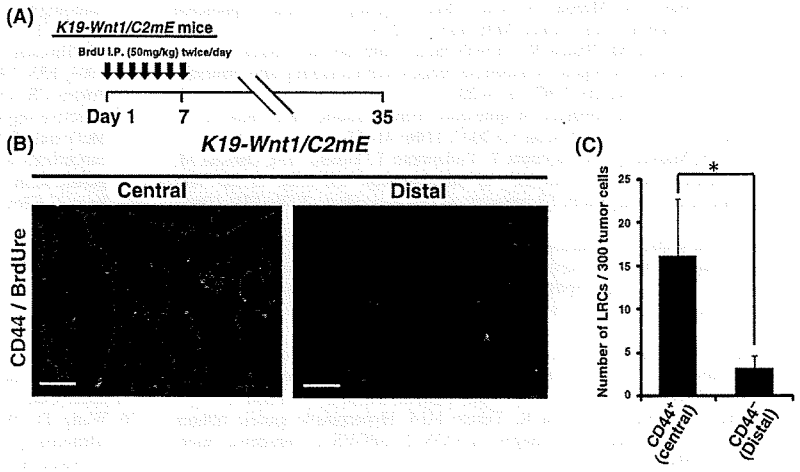

Fig. 4. Slow-cycling CD44$^+$ cells in *K19-Wnt1/C2mE* mice. (A) The protocol of long-term BrdU label-retaining assay using *K19-Wnt1/C2mE* mice. (B) Immunofluorescence analysis of double staining for BrdU label-retaining/CD44 in gastric tumors of 30-week-old *K19-Wnt1/C2mE* mice. Scale bars = 50 μm. (C) Number of label-retaining cells in CD44$^+$ tumor cells at the central region or CD44$^-$ tumor cells in the periphery of gastric tumors, respectively. Data are means ± SD from four microscopic fields. *$P < 0.01$.

Therefore, we assumed that the CD44$^+$ slow-cycling cells in the normal stomach SCJ would be candidates for the cell-of-origin of gastric CSCs in *K19-Wnt1/C2mE* mice.

The normal gastric stem/progenitor cells are thought to be located in the isthmus/neck region of gastric glands.[21] It is not known whether the SCJ region of mice stomach, which

corresponds to human EC junction, contains gastric stem/progenitor cells. However, both the human EC junction and mouse SCJ region are common sites of tumor development.[18,25] Based on this evidence and our present study, we presume that these junctional regions in human and mouse might contain stem/progenitor cells that expand in response to the activation of PGE_2-mediated signaling and give rise to gastric tumor, although further investigations are needed to support this concept. Furthermore, we found large numbers of $CD44^+$ gastric glands in human adenocarcinomas and adjacent metaplasias, but not in the normal gastric epithelium (data not shown). Thus, it is possible that a few $CD44^+$ stem-like cells, similar to the mouse SCJ cells, reside in human normal gastric epithelium and that metaplastic changes, often triggered by chronic inflammation, are induced by the expansion of $CD44^+$ stem-like cells through the activation of PGE_2 signaling.

PGE_2, an inflammatory mediator released at the site of tissue inflammation, promotes colon adenoma growth in *APC* mutant mice,[26] and triggers the expansion of hematopoietic stem cells.[23] These observations suggest that PGE_2 and its downstream signaling effectors potentiate the self-renewal ability of stem/progenitor cells *in vivo*. Importantly, we previously reported that tumor necrosis factor-α, a mediator of PGE_2-induced inflammatory signaling, triggers sustained proliferation of progenitor cells in gastric tumors of *K19-C2mE* mice.[10] Therefore, PGE_2 and its downstream targets might play key roles in the regulation of $CD44^+$ slow-cycling cell expansion.

Aberrant activation of Wnt signaling, which regulates the self-renewal of stem/progenitor cells, has been shown to trigger colon tumorigenesis.[22] In the present study, we found that the activation of Wnt signaling alone is not sufficient for $CD44^+$ SCJ cell expansion in the absence of PGE_2 signaling, as seen in *K19-Wnt1* mice. In contrast, Wnt signaling cooperatively promotes PGE_2-induced $CD44^+$ gland cell expansion in *K19-Wnt1/C2mE* mice. These results indicate that Wnt signaling stimulates the proliferation of $CD44^+$ stem-like cells during inflammation, leading to the enhancement of PGE_2-induced expansion of $CD44^+$ quiescent or slow-cycling cells in gastric tumorigenesis.

It is important to note that $CD44^+$ cells in the normal SCJ gland were LRCs and/or $Ki67^-$ cells (Fig. 2B), suggesting that CD44 expression is related to quiescent or slow-cycling characteristics in normal stem cells. However, in the glands expanded by the cooperative activation of PGE_2 and Wnt, CD44 expression was found not only in LRCs and $Ki67^-$ cells but also in some $Ki67^+$ cycling cells (data not shown). These findings indicate that CD44 expression does not strictly correlate with the quiescent or slow-cycling status in the context of cancer cells. Further investigations on the functional association of CD44 with various cell cycle regulators in both normal and cancer cells are warranted.

Taken together, our present findings suggest that the eradication of the $CD44^+$ subpopulation consisting of quiescent or slow-cycling cells and the suppression of Wnt/PGE_2-mediated $CD44^+$ cell expansion would be an interesting strategy for the development of efficient therapies against gastric cancers.

Acknowledgments

We thank I. Ishimatsu, N. Suzuki, and Y. Ito for technical assistance, K. Arai for help in preparation of the manuscript, and M. Miyasaka for providing the anti-pan-CD44 antibody (IM7). This work was supported by grants from the Ministry of Education, Culture, Sports, Science, and Technology of Japan (to O.N. and H.S.).

References

1 Ponta H, Sherman L, Herrlich PA. CD44: from adhesion molecules to signalling regulators. *Nat Rev* 2003; **4**: 33–45.
2 Aruffo A, Stamenkovic I, Melnick M, Underhill CB, Seed B. CD44 is the principal cell surface receptor for hyaluronate. *Cell* 1990; **61**: 1303–13.
3 Visvader JE, Lindeman GJ. Cancer stem cells in solid tumours: accumulating evidence and unresolved questions. *Nat Rev Cancer* 2008; **8**: 755–68.
4 Takaishi S, Okumura T, Tu S *et al.* Identification of gastric cancer stem cells using the cell surface marker CD44. *Stem Cells* 2009; **27**: 1006–20.
5 Zabierowski SE, Herlyn M. Melanoma stem cells: the dark seed of melanoma. *J Clin Oncol* 2008; **26**: 2890–4.
6 Ito K, Bernardi R, Morotti A *et al.* PML targeting eradicates quiescent leukaemia-initiating cells. *Nature* 2008; **453**: 1072–8.
7 Holtz M, Forman SJ, Bhatia R. Growth factor stimulation reduces residual quiescent chronic myelogenous leukemia progenitors remaining after imatinib treatment. *Cancer Res* 2007; **67**: 1113–20.
8 Arai F, Suda T. Maintenance of quiescent hematopoietic stem cells in the osteoblastic niche. *Ann N Y Acad Sci* 2007; **1106**: 41–53.
9 Oshima H, Matsunaga A, Fujimura T, Tsukamoto T, Taketo MM, Oshima M. Carcinogenesis in mouse stomach by simultaneous activation of the Wnt signaling and prostaglandin E2 pathway. *Gastroenterology* 2006; **131**: 1086–95.
10 Oshima M, Oshima H, Matsunaga A, Taketo MM. Hyperplastic gastric tumors with spasmolytic polypeptide-expressing metaplasia caused by tumor necrosis factor-alpha-dependent inflammation in cyclooxygenase-2/microsomal prostaglandin E synthase-1 transgenic mice. *Cancer Res* 2005; **65**: 9147–51.
11 Okamoto I, Morisaki T, Sasaki J *et al.* Molecular detection of cancer cells by competitive reverse transcription-polymerase chain reaction analysis of specific CD44 variant RNAs. *J Natl Cancer Inst* 1998; **90**: 307–15.
12 Oshima H, Oshima M, Inaba K, Taketo MM. Hyperplastic gastric tumors induced by activated macrophages in COX-2/mPGES-1 transgenic mice. *EMBO J* 2004; **23**: 1669–78.
13 Tanabe KK, Ellis LM, Saya H. Expression of CD44R1 adhesion molecule in colon carcinomas and metastases. *Lancet* 1993; **341**: 725–6.
14 Mayer B, Jauch KW, Gunthert U *et al.* De-novo expression of CD44 and survival in gastric cancer. *Lancet* 1993; **342**: 1019–22.
15 Miwa T, Watanabe A, Yamada Y *et al.* Progression in gastric carcinoma relative to the ratio of CD44 epithelial variant transcript to CD44 hematopoietic variant transcript. *Cancer* 1996; **77**: 25–9.
16 Zou GM. Cancer initiating cells or cancer stem cells in the gastrointestinal tract and liver. *J Cell Physiol* 2008; **217**: 598–604.
17 Hollingsworth MA, Swanson BJ. Mucins in cancer: protection and control of the cell surface. *Nat Rev Cancer* 2004; **4**: 45–60.
18 Odze RD. Unraveling the mystery of the gastroesophageal junction: a pathologist's perspective. *Am J Gastroenterol* 2005; **100**: 1853–67.
19 Qiao XT, Ziel JW, McKimpson W *et al.* Prospective identification of a multilineage progenitor in murine stomach epithelium. *Gastroenterology* 2007; **133**: 1989–98.
20 Potten CS, Owen G, Booth D. Intestinal stem cells protect their genome by selective segregation of template DNA strands. *J Cell Sci* 2002; **115**: 2381–8.
21 McDonald SA, Greaves LC, Gutierrez-Gonzalez L *et al.* Mechanisms of field cancerization in the human stomach: the expansion and spread of mutated gastric stem cells. *Gastroenterology* 2008; **134**: 500–10.
22 Reya T, Clevers H. Wnt signalling in stem cells and cancer. *Nature* 2005; **434**: 843–50.
23 North TE, Goessling W, Walkley CR *et al.* Prostaglandin E2 regulates vertebrate haematopoietic stem cell homeostasis. *Nature* 2007; **447**: 1007–11.
24 Goessling W, North TE, Loewer S *et al.* Genetic interaction of PGE2 and Wnt signaling regulates developmental specification of stem cells and regeneration. *Cell* 2009; **136**: 1136–47.
25 Bleuming SA, He XC, Kodach LL *et al.* Bone morphogenetic protein signaling suppresses tumorigenesis at gastric epithelial transition zones in mice. *Cancer Res* 2007; **67**: 8149–55.
26 Wang D, Wang H, Shi Q *et al.* Prostaglandin E(2) promotes colorectal adenoma growth via transactivation of the nuclear peroxisome proliferator-activated receptor delta. *Cancer Cell* 2004; **6**: 285–95.

doi: 10.1111/j.1349-7006.2009.01430.x

Cancer Science
The official journal of the Japanese Cancer Association JCA

Review Article

Prostaglandin E_2, Wnt, and BMP in gastric tumor mouse models

Hiroko Oshima, Keisuke Oguma, Yu-Chen Du and Masanobu Oshima[1]

Division of Genetics, Cancer Research Institute, Kanazawa University, Takara-machi, Kanazawa, Japan

(Received May 26, 2009/Revised June 13, 2009/Accepted June 15, 2009/Online publication July 20, 2009)

The development of gastric cancer is closely associated with *Helicobacter pylori* (*H. pylori*) infection. The expression of cylooxigenase-2 (COX-2), a rate-limiting enzyme for prostaglandin biosynthesis, is induced in *H. pylori*-associated chronic gastritis, which thus results in the induction of proinflammatory prostaglandin, PGE_2. The COX-2/PGE_2 pathway plays a key role in gastric tumorigenesis. On the other hand, several oncogenic pathways have been shown to trigger gastric tumorigenesis. The activation of Wnt/β-catenin signaling is found in 30–50% of gastric cancers, thus suggesting that Wnt signaling plays a causal role in gastric cancer development. Mutations in the bone morphogenetic protein (BMP) signaling pathway are responsible for the subset of juvenile polyposis syndrome (JPS) that develops hamartomas in the gastrointestinal tract. BMP suppression appears to contribute to gastric cancer development because gastric cancer risk is increased in JPS. Wnt signaling is important for the maintenance of gastrointestinal stem cells, while BMP promotes epithelial cell differentiation. Accordingly, it is possible that both Wnt activation and BMP suppression can cause gastric tumorigenesis through enhancement of the undifferentiated status of epithelial cells. Recent mouse model studies have indicated that induction of the PGE_2 pathway is required for the development of both gastric adenocarcinoma and hamartoma in the Wnt-activated and BMP-suppressed gastric mucosa, respectively. This article reviews the involvement of the PGE_2, Wnt, and BMP pathways in the development of gastric cancer, and gastric phenotypes that are found in transgenic mouse models of PGE_2 induction, Wnt activation, BMP suppression, or a combination of these pathways. (*Cancer Sci* 2009; 100: 1779–1785)

Epidemiological studies indicate that the regular use of nonsteroidal anti-inflammatory drugs (NSAIDs) lowers the mortality rate of gastrointestinal cancer.[1] The major target of NSAIDs is cyclooxygenases (COXs), COX-1 and COX-2, which are rate-limiting enzymes for prostaglandin biosynthesis (Fig. 1). COX-1 is constitutively expressed in most tissues and it is considered to be responsible for physiological levels of prostaglandin.[2] In contrast, COX-2 is induced in inflammation by various stimuli including cytokines and growth factors.[3–5] The induction of COX-2 expression is also found in a variety of cancer tissues. Mouse genetic studies have demonstrated that disruption of the *Ptgs2* gene encoding COX-2 results in the suppression of tumor development in the intestine and skin.[6,7] Moreover, various animal studies have confirmed that treatment with NSAIDs or COX-2 selective inhibitors (COXIBs) suppressed chemically induced tumor formation and xenografted tumor growth.[8] These results, taken together, indicate that the COX-2 pathway plays an essential role in cancer development.

However, the mechanism of the COX-2 pathway underlying gastric tumorigenesis has not yet been fully elucidated. To investigate the possible crosstalk between the COX-2 pathway and oncogenic activation in gastric carcinogenesis, a series of mouse models have been constructed and examined as discussed in this review.

Induction of the COX-2/PGE_2 pathway in gastric cancer

Regular use of NSAIDs is associated with a decreased incidence of gastric cancer.[9–12] Induction of COX-2 is found in approximately 70% of gastric cancer, whereas the expression of COX-1 is not elevated.[13,14] Gastric cancer can be divided into two histological subtypes: intestinal and diffuse types, and the expression of COX-2 is found predominantly in the intestinal-type gastric cancer.[15] These results suggest that the COX-2 pathway plays a role in the development of intestinal-type gastric cancer.

Infection with *Helicobacter pylori* (*H. pylori*) causes chronic gastritis, which is associated with gastric carcinogenesis.[16] The expression of COX-2 is significantly induced in the *H. pylori*-infected gastric mucosa, and that COX-2 expression is suppressed by the eradication of *H. pylori*.[17] Although the molecular mechanism for COX-2 induction in tumors has not been elucidated, it is possible that the cytokine network is activated by infection and induces the expression of COX-2. *H. pylori* can stimulate Toll-like receptors (TLRs), leading to activation of the nuclear factor-κB (NF-κB) pathway that induces the expression of COX-2 (Fig. 1).[18,19] Moreover, TLR2/TLR9 signaling by *H. pylori* activates mitogen activated protein kinases (MAPK) including p38, resulting in the activation of CRE and AP-1 elements on the COX-2 gene promoter.[19,20]

Microsomal PGE synthase-1 (mPGES-1), a PGE_2 converting enzyme is functionally coupled with COX-2.[21] Simultaneous induction of COX-2 and mPGES-1 is observed in gastric cancer tissues suggesting induction of the PGE_2 pathway in gastric tumors (Fig. 1).[22,23] The level of mPGES-1 also decreases after the eradication of *H. pylori*,[24] thus indicating that *H. pylori* infection induces the PGE_2 pathway through induction of both COX-2 and mPGES-1. The PGE_2 level significantly increases in gastric cancer,[25] and the level is associated with the *H. pylori* infection status.[26]

Gastric tumor development in mouse and rat models induced by chemical carcinogens or *Helicobacter* infection is suppressed by treatment with NSAIDs or COXIBs.[27–29] *H. pylori* infection in Mongolian gerbils induces gastric tumorigenesis, which is quite similar to the course of human gastric carcinogenesis. Importantly, treatment with *H. pylori*-infected and chemical carcinogen-treated Mongolian gerbils with a COXIB suppressed gastric carcinogenesis.[30,31] These animal studies suggest that the COX-2 pathway thus plays an essential role in *H. pylori* infection–associated gastric tumorigenesis.

[1]To whom correspondence should be addressed.
E-mail: oshimam@kenroku.kanazawa-u.ac.jp

doi: 10.1111/j.1349-7006.2009.01258.x

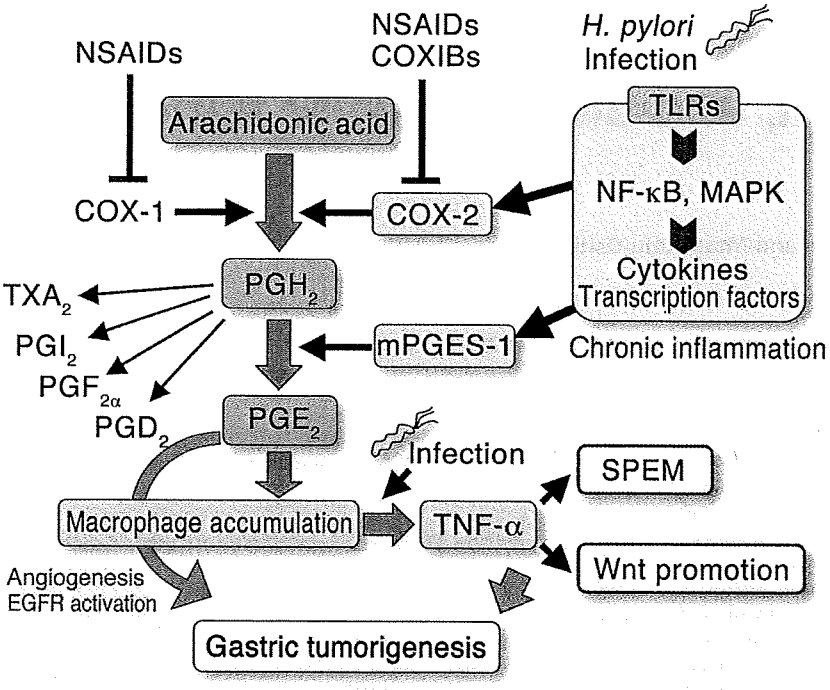

Fig. 1. Schematic presentation of arachidonic acid metabolism in the context of gastric tumorigenesis. The expression of cyclooxygenase (COX)-2 and microsomal PGE synthase-1 (mPGES-1) is induced by *Helicobacter pylori* (*H. pylori*)-associated inflammatory responses. The simultaneous expression of both COX-2 and mPGES-1 leads to induction of the prostaglandin PGE_2 pathway, which results in macrophage accumulation. These macrophages are activated by infectious stimuli, resulting in the induction of tumor necrosis factor (TNF)-α-dependent SPEM development and the promotion of Wnt signaling, which may contribute to gastric tumorigenesis. The induction of angiogenesis and activation of epidermal growth factor receptor (EGFR) signaling are also possible mechanisms of PGE_2 in tumorigenesis. COXIBs, COX-2 selective inhibitors; NF-κB, nuclear factor-κB; NSAIDS, nonsteroidal anti-inflammatory drugs; SPEM, spasmolytic polypeptide/TFF2-expressing metaplasia; TLRs, Toll-like receptors.

K19-C2mE transgenic mice: A model for PGE_2 induction in the stomach

K19-C2mE transgenic mice express both COX-2 and mPGES-1 in gastric epithelial cells, which results in induction of the PGE_2 pathway in the stomach (Fig. 2).[32] *K19-C2mE* mice develop hyperplastic lesions in the glandular stomach. Histologically, the major cell type of hyperplasia is the mucous cell, which is similar to that found in the spasmolytic polypeptide/TFF2-expressing metaplasia (SPEM; Fig. 2).[33] The development of SPEM is associated with an *H. pylori* infection and gastric adenocarcinoma, thus suggesting that SPEM is an *H. pylori*-induced precancerous lesion.[34] It is thus possible that the PGE_2 pathway induced by *H. pylori* infection is responsible for the development of SPEM. Treatment with *N*-methyl-*N*-nitrosourea (MNU) to the *H. pylori*-infected mice causes gastric tumor development. Notably, the multiplicity of gastric tumors induced by *H. pylori* infection and MNU treatment was significantly higher in *K19-C2mE* mice compared with wild-type mice.[35] These results suggest that PGE_2-induced metaplastic hyperplasia is a precursor for chemical carcinogen-induced gastric tumor.

Notably, macrophages infiltrate and are activated in the gastric mucosa of *K19-C2mE* mice.[32] The activation of these macrophages is suppressed by treatment with antibiotics, thus indicating that infectious stimuli activate the accumulated macrophages. Importantly, the development of SPEM is also suppressed by antibiotic treatment, thus suggesting that bacterial infection activates macrophages, which is required for SPEM development. Consistently, disruption of the tumor necrosis factor (*TNF*)-α gene in *K19-C2mE* mice results in the suppression of SPEM development, thus suggesting that TNF-α derived from activated macrophages plays an essential role in SPEM formation.[33] Moreover, it is conceivable that the induction of PGE_2 signaling is the primary cause for the mucosal macrophage accumulation, because the treatment of *K19-C2mE* mice with a COXIB, but not with antibiotics, inhibits macrophage infiltration. A possible mechanism for the processes from *H. pylori* infection to SPEM development through PGE_2 induction and macrophage activation is depicted in Figure 1.

Activation of Wnt signaling in gastric cancer

Canonical Wnt signaling (Wnt/β-catenin signaling) is a critical pathway in the regulation of development as well as in tumorigenesis.[36] In the absence of the Wnt ligand, cytoplasmic β-catenin is phosphorylated by GSK-3β within a complex containing adenomatous polyposis coli (APC) and Axin, thus resulting in the degradation of β-catenin through the ubiquitin proteasome pathway.[37] When Wnt ligands bind Frizzled receptors, phosphorylation of β-catenin is suppressed, leading to stabilization and nuclear translocation of β-catenin (Fig. 3). Nuclear β-catenin interacts with T-cell factor/lymphocyte enhancer factor (TCF/LEF) to induce transcription of Wnt target genes. *APC* or β-catenin mutation causes tumor development by activation of the canonical Wnt signaling.

Patients with germ-line mutations in the *APC* gene have an increased risk of gastric cancer.[38] Moreover, β-catenin accumulation, a hallmark of Wnt activation, is found in 30–50% of gastric cancers.[39,40] These results suggest that Wnt activation is one of the major causes of gastric cancer development. In gastric cancer, mutations in β-catenin are reported, while *APC* mutations are rarely detected.[41–43] However, the incidence of β-catenin mutations is less than 30% in the Wnt-activated gastric cancers,[39] thus suggesting mechanism(s) other than *APC* or β-catenin mutation for activation of the Wnt pathway. It has been suggested that the cytoplasmic β-catenin level is increased by E-cadherin downregulation or β-TrCP mutation through decrease of E-cadherin-bound membrane β-catenin or inhibition of β-catenin ubiquitination, respectively (Fig. 3).[44,45] These mechanisms may thus contribute to the activation of Wnt signaling in gastric tumorigenesis. On the other hand, the expression of the *SFRP1*, *-2*, and *-5* genes are silenced by promoter methylation in gastric cancer cells.[46] SFRPs are secreted endogenous antagonist of the Wnt ligands. Accordingly, it is possible that *SFRP* methylation is also an

doi: 10.1111/j.1349-7006.2009.01258.x

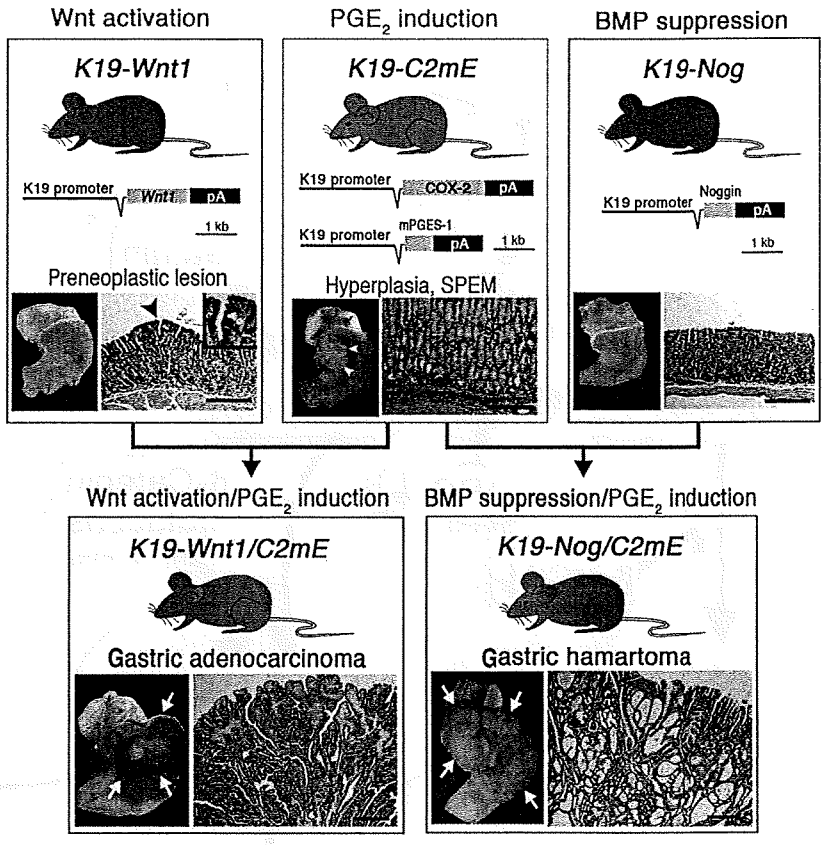

Fig. 2. Transgenic mouse models of gastric tumorigenesis. Transgenic vector construction(s) and representative macroscopic and microscopic photographs of the stomach are shown for each line. *K19-Wnt1/C2mE* and *K19-Nog/C2mE* are compound transgenic mice of *K19-Wnt1* and *K19-C2mE*, and *K19-Nog* and *K19-C2mE*, respectively. The arrowhead in the *K19-Wnt1* mouse stomach indicates a preneoplastic lesion. The arrowheads and asterisks in the *K19-C2mE* mouse stomach indicate gastric hyperplasia and mucous metaplasia (SPEM), respectively. The arrows in *K19-Wnt1/C2mE* and *K19-Nog/C2mE* indicate gastric tumors. Note that the histology of the *K19-Wnt1/C2mE* mouse shows dysplastic adenocarcinoma, while that of the *K19-Nog/C2mE* mouse shows hamartoma with dilated cystic structure. Bars indicate 100 μm. (Reproduced from Oshima *et al. Cancer Res*, 69: 2729–33, 2009.) BMP, bone morphogenetic protein; COX-2, cyclooxygenase-2; SPEM, spasmolytic polypeptide/TFF2-expressing metaplasia.

important mechanism for Wnt activation in gastric tumorigenesis (Fig. 3).[46]

K19-Wnt1 transgenic mice: A model for Wnt activation in the stomach

K19-Wnt1 transgenic mice express Wnt1, one of the canonical Wnt ligands, in the gastric epithelial cells, which results in the activation of Wnt signaling in the stomach (Fig. 2).[40] The number of undifferentiated epithelial cells increases in the *K19-Wnt1* mouse stomach, thus suggesting that Wnt signaling keeps gastric epithelial cells in an undifferentiated status. Small preneoplastic lesions spontaneously develop in the gastric mucosa of *K19-Wnt1* mice, which consist of dysplastic epithelial cells (Fig. 2). However, gastric tumors do not develop in *K19-Wnt1* mice. It is thus possible that the activation of Wnt signaling can trigger tumorigenesis and form small preneoplastic lesions; however, Wnt activation alone is not sufficient for tumor development (Fig. 3).

To examine the effect of the PGE_2 pathway in the Wnt-activated gastric mucosa, *K19-Wnt1* mice were crossed with *K19-C2mE* to construct compound transgenic mice (*K19-Wnt1/C2mE* mice), in which both the Wnt and PGE_2 pathways were activated in the stomach simultaneously. Importantly, *K19-Wnt1/C2mE* mice developed gastric adenocarcinoma (Fig. 2).[40] The tumors consisted of dysplastic epithelial cells, which sometimes invade the smooth muscle layers. These results clearly indicate that the simultaneous activation of the Wnt and PGE_2 pathways is responsible for the development of gastric adenocarcinomas. Importantly, the gene expression profile of *K19-Wnt1/C2mE* mouse gastric tumors is similar to that of human intestinal-type gastric cancer (Hiraku Itadani *et al.*, submitted manuscript, 2009). Therefore, *K19-Wnt1/C2mE* mice recapitulate human intestinal-type gastric cancer not only in the molecular etiology, but also in the pathological and molecular characteristics of tumors.

These results of mouse model studies suggest the following possible scenario for gastric tumorigenesis (Fig. 3): *H. pylori* infection causes the induction of the COX-2/PGE_2 pathway, which thus leads to SPEM development. The activation of Wnt signaling in the normal gastric mucosa causes small preneoplastic lesions, but is not sufficient for tumor formation. When Wnt signaling is activated in the PGE_2 induction–associated inflamed mucosa, gastric adenocarcinomas develop through cooperation of the Wnt and PGE_2 pathways.

Suppression of BMP signaling in gastric tumors

Juvenile polyposis syndrome (JPS) is characterized by hereditary gastrointestinal hamartomatous polyposis,[47] a subset of which is caused by germline mutations in the BMP receptor type IA gene (*BMPR1A*).[48] BMP ligands bind to a complex of the BMP receptor type II and I, leading to phosphorylation of Smad1,5,8, thereby allowing them to form a complex with Smad4.[49,50] These Smad complexes translocate to the nuclei and function as transcription enhancers. BMP signaling inhibits epithelial proliferation and promotes differentiation.[51,52] The suppression of BMP signaling in the mouse intestine results in hamartomatous polyp development,[52,53] elongated villi, and crypt fission.[54] These results suggest that the suppression of BMP signaling causes tumorigenesis by the inhibition of epithelial cell differentiation. Although the main affected site in JPS patients is the intestine, gastric polyps also develop in JPS, and the cancer risk in JPS patients increases both in the colon and stomach.[55,56] Moreover, the expression of BMP-2 is suppressed by promoter methylation

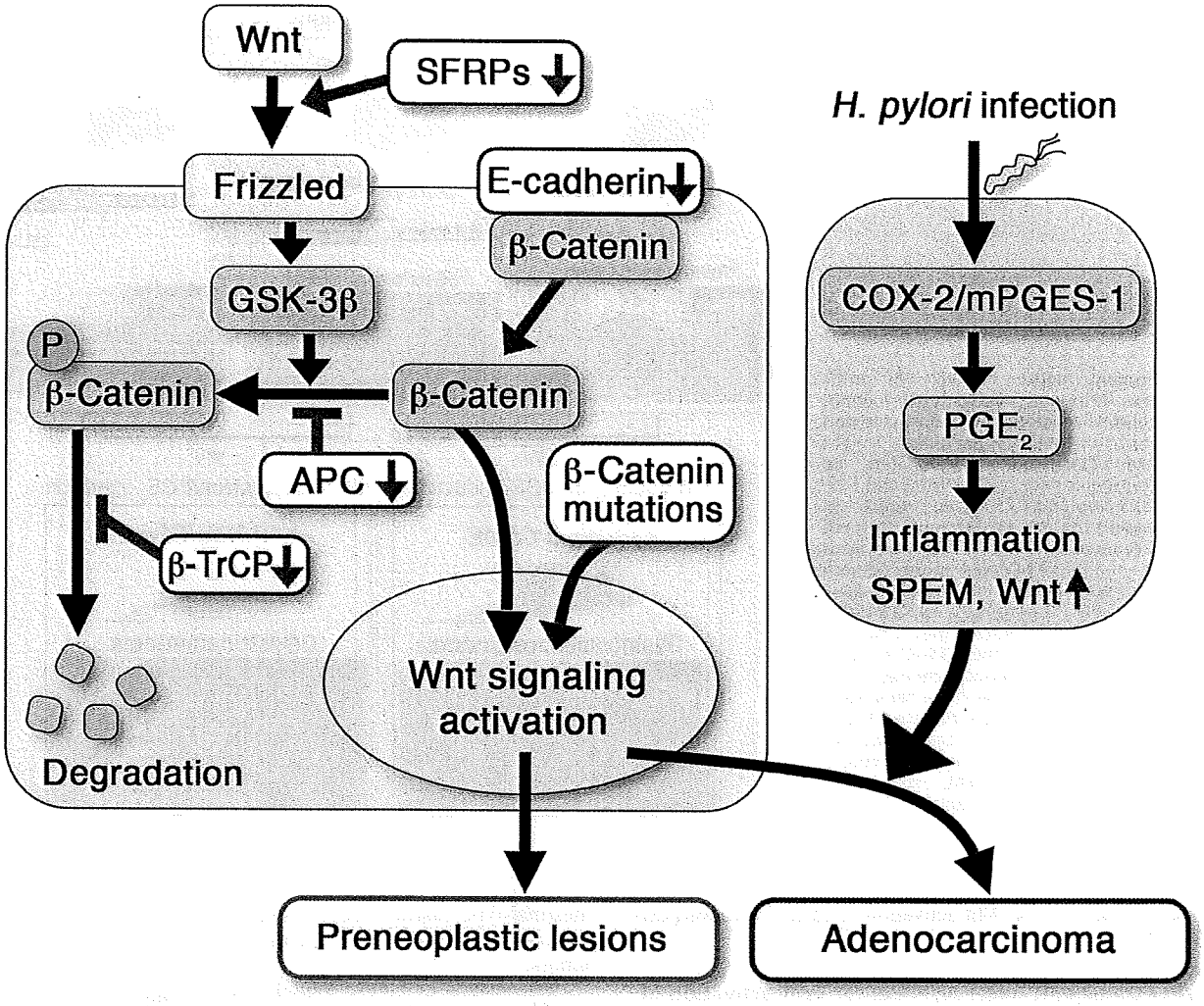

Fig. 3. Schematic presentation of the canonical Wnt signaling and cyclooxygenase (COX)-2/prostaglandin PGE_2 pathway in gastric tumor development. β-Catenin mutations, *SFRPs* methylation, and downregulation of E-cadherin or β-TrCP can activate Wnt signaling in gastric cancer. Cooperation of the *Helicobacter pylori* (*H. pylori*)-induced COX-2/PGE_2 pathway with Wnt activation leads to the development of gastric adenocarcinoma. Without the induction of the PGE_2 pathway, Wnt activation alone does not cause gastric cancer development. mPGES-1, microsomal PGE synthase-1.

in gastric cancer cells,[57] and stimulation of gastric cancer cells with BMP-2 suppresses proliferation.[58] These results suggest that the inhibition of BMP signaling contributes to gastric tumorigenesis through the suppression of differentiation.

K19-Nog transgenic mice: A model for BMP suppression in the stomach

K19-Nog mice express noggin, an endogenous BMP antagonist, in the gastric epithelial cells, thus resulting in the inhibition of BMP signaling in the stomach (Fig. 2).[59] Noggin is a polypeptide that inhibits BMP signaling by binding the BMP ligands.[50] In the *K19-Nog* mice, the phosphorylation of Smad1,5,8 is suppressed in the gastric gland by BMP inhibition. However, *K19-Nog* mice do not develop gastric lesions, and the histology of the gastric mucosa is normal (Fig. 2). To examine the effect of cooperation of BMP suppression and PGE_2 induction, *K19-Nog* mice were crossed with *K19-C2mE* to construct compound transgenic mice (*K19-Nog/C2mE* mice), in which BMP signaling is suppressed and the PGE_2 pathway is induced in the gastric mucosa. Importantly, *K19-Nog/C2mE* mice develop large tumors in the glandular stomach (Fig. 2). These results indicate that the suppression of BMP signaling is insufficient for gastric tumorigenesis; however, the induction of the PGE_2 pathway does promote tumor formation in the BMP-suppressed gastric mucosa.

Histologically, *K19-Nog/C2mE* mouse tumors are not dysplastic, but consist of irregular branching of epithelial cell layers, combined with dilated cysts (Fig. 2). Such histological characteristics are distinct from adenocarcinomas of *K19-Wnt1/C2mE* mice, but are typical of the hamartomas of JPS patients.[55,56,60] These results indicate that the suppression of BMP signaling associated with PGE_2 induction causes gastric hamartoma development. Accordingly, it is possible that types of genetic alterations determine the histological types of tumors, e.g. adenocarcinoma by Wnt activation or hamartoma by BMP suppression. Furthermore, the induction of the PGE_2 pathway promotes tumor formation regardless of the histological types (Fig. 2). Accordingly, it is thus possible that *H. pylori* infection contributes to development of both types of gastric tumors through PGE_2 induction.

It has been reported that BMP signaling negatively regulates Wnt signaling in the intestinal crypt.[53] Namely, suppression of BMP signaling enhances Wnt activity through the activation of PI3K/Akt pathway. However, the β-catenin level in the *K19-Nog/C2mE* hamartomas is the same as that in the wild-type

doi: 10.1111/j.1349-7006.2009.01258.x

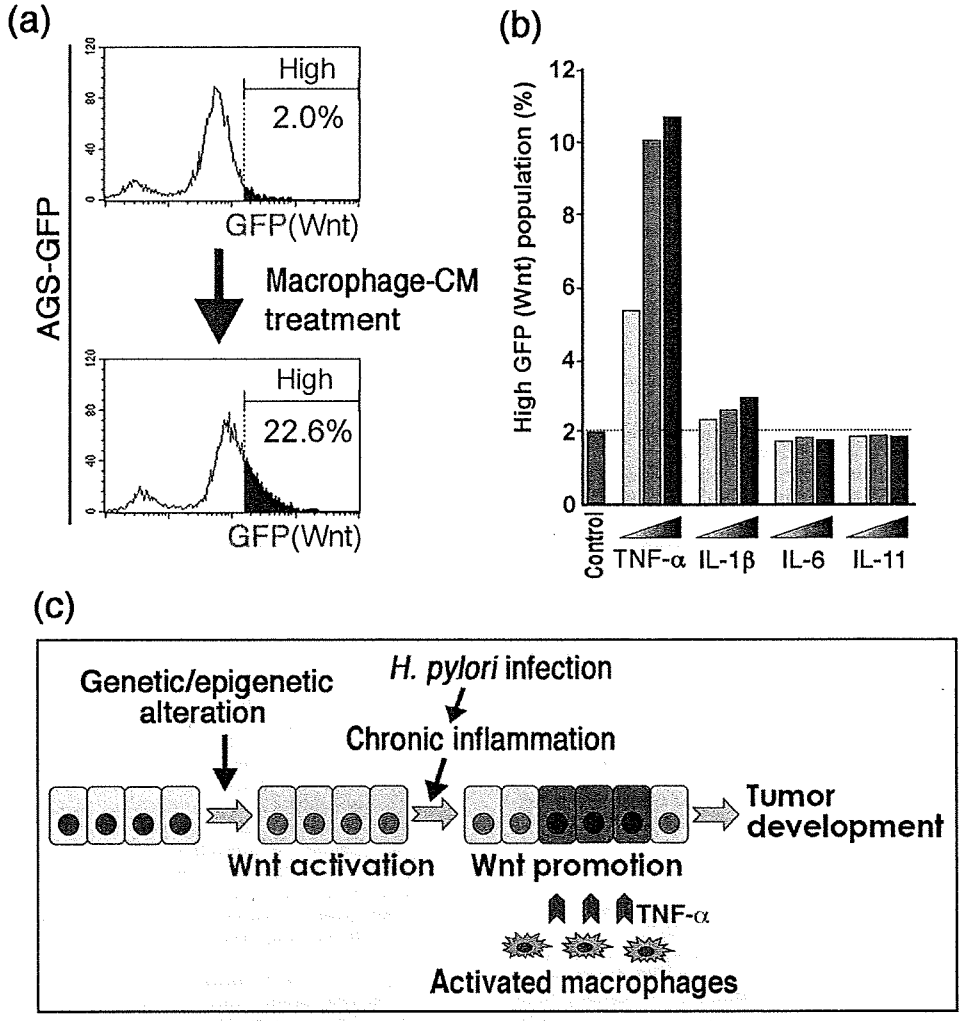

Fig. 4. Promotion of Wnt signaling by macrophage-derived tumor necrosis factor (TNF)-α in gastric cancer cells. (a) Representative FACS analyses of Wnt-reporter gastric cancer cells, AGS-GFP, in which GFP expression is regulated by β-catenin/TCF. GFP intensity increased significantly when cells were treated with conditioned medium (CM) from activated macrophages. (b) GFP intensity of reporter cells treated with indicated cytokines are shown in the bar graph. Note that Wnt activity is elevated by treatment with TNF-α in a dose-dependent manner. (c) Hypothesis for gastric tumor development. The level of Wnt signaling activated by genetic/epigenetic alteration is not sufficient for tumorigenesis. However, *Helicobacter pylori* (*H. pylori*) infection-induced inflammation promotes the Wnt activation level through macrophage-derived TNF-α, which contributes to gastric tumorigenesis. (a and b, reproduced from Oguma *et al. EMBO J*, 27: 1671–81, 2008, with permission from the Nature Publishing Group.)

mouse stomach, while it is markedly elevated in *K19-Wnt1/C2mE* gastric tumors.[59] These results indicate that gastric hamartomas develop in *K19-Nog/C2mE* mice due to a Wnt-activation independent mechanism.

Possible mechanisms of the PGE_2 pathway in gastric tumorigenesis

There are four G protein-coupled receptors for PGE_2, EP1–EP4. Among these receptors, the expression of EP4 increased significantly in gastric tumors of both *K19-Wnt1/C2mE* mice and *K19-Nog/C2mE* mice.[59] It is thus possible that PGE_2 signaling through EP4 plays a role in the development of adenocarcinoma and hamartoma in the Wnt-activated and BMP-suppressed gastric mucosa, respectively.

The promotion of the Wnt signaling activity beyond the basal activation level may be important for malignant progression.[61] For example, increased accumulation of β-catenin is found in the invasion front of colon cancer, suggesting that the increased Wnt activation level contributes to tumor invasion.[62] Hepatocyte growth factor (HGF) and platelet-derived growth factor (PDGF) increase the Wnt signaling activity in colon cancer cells, suggesting that these factors function as Wnt promoters.[63,64] Notably, the level of Wnt signaling activity in gastric cancer cells significantly increases when the cells are stimulated with a conditioned medium from activated macrophages (Fig. 4a).[65] Moreover, TNF-α, but not other proinflammatory cytokines, caused an increase in the Wnt signaling activity in gastric cancer cells (Fig. 4b).[65] These results suggest the hypothesis that Wnt activation, due to either genetic or epigenetic alterations in normal epithelial cells, is not sufficient for gastric tumor development. However, the Wnt activation level increases further in the inflamed mucosa by macrophage-derived TNF-α, and such Wnt promotion contributes to gastric cancer development (Fig. 4c). The induction of the PGE_2 pathway leads to macrophage accumulation in the gastric mucosa. It is therefore conceivable that the induction of Wnt promotion is one of the important mechanisms of the PGE_2 pathway in gastric tumorigenesis (Fig. 1).

Conclusions

Studies with mouse models have elucidated the roles of the PGE_2 pathway in gastric tumorigenesis in the Wnt-activated and BMP-suppressed gastric mucosa. Alterations in morphogen signals, such as the Wnt and BMP pathways, can therefore trigger gastric tumorigenesis by the suppression of epithelial differentiation. However, alterations of these signals in the non-inflamed stomach do not cause gastric tumor formation. In contrast, alterations of these signals in the inflamed gastric mucosa lead to the development of gastric tumors through cooperation with the PGE_2 pathway. Moreover, mouse studies show the possible mechanisms of PGE_2 in gastric tumorigenesis, i.e. macrophage accumulation and activation, subsequent SPEM formation, and Wnt signaling promotion. Considering the multifunctional nature of PGE_2, it is possible that other mechanisms triggered by the PGE_2 pathway may also contribute to gastric tumorigenesis, which should be further elucidated using mouse models in the future. These studies will provide a rationale for the inhibition of the PGE_2 pathway as a possible preventative strategy against gastric tumorigenesis.

Acknowledgment

We thank Manami Watanabe for her helpful work with the papers that we cited in this review article.

References

1 Thun MJ, Namboodiri MM, Heath CW Jr. Aspirin use and reduced risk of fatal colon cancer. *N Engl J Med* 1991; **325**: 1593–6.
2 Dewitt DL, Smith WL. Primary structure of prostaglandin G/H synthase from sheep vesicular gland determined from the complementary DNA sequence. *Proc Natl Acad Sci USA* 1998; **85**: 1412–6.
3 Xie WL, Chipman JG, Robertson DL, Erikson RL, Simmons DL. Expression of a mitogen-responsive gene encoding prostaglandin synthase is regulated by mRNA splicing. *Proc Natl Acad Sci USA* 1991; **88**: 2692–6.
4 Fletcher BS, Kujubu DA, Perrin DM, Herschman HR. Structure of the mitogen-inducible TIS10 gene and demonstration that the TIS10-encoded protein is a functional prostaglandin G/H synthase. *J Biol Chem* 1992; **267**: 4338–44.
5 Hla T, Neilson K. Human cylooxygenase-2 cDNA. *Proc Natl Acad Sci USA* 1992; **89**: 7384–8.
6 Oshima M, Dinchuk JE, Kargman SL *et al.* Suppression of intestinal polyposis in *Apc*$^{\Delta 716}$ knockout mice by inhibition of cyclooxygenase 2 (COX-2). *Cell* 1996; **87**: 803–9.
7 Chulada PC, Thompson MB, Mahler JF *et al.* Genetic disruption of Ptgs-1, as well as Ptgs-2, reduces intestinal tumorigenesis in Min mice. *Cancer Res* 2000; **60**: 4705–8.
8 Oshima M, Taketo MM. COX selectivity and animal models for colon cancer. *Curr Pharm Des* 2002; **8**: 1021–34.
9 Thun MJ, Namboodiri MM, Calle EE, Flanders WD, Heath CW Jr. Aspirin use and risk of fatal cancer. *Cancer Res* 1993; **53**: 1322–7.
10 Schreinemachers DM, Everson RB. Aspirin use and lung, colon, and breast cancer incidence in a prospective study. *Epidemiology* 1994; **5**: 138–46.
11 Zaridze D, Borisova E, Maximovitch D, Chkhikvadze V. Aspirin protects against gastric cancer: results of a case-control study from Moscow, Russia. *Int J Cancer* 1999; **82**: 473–6.
12 Akre K, Ekstrom AM, Signorello LB, Hansson LE, Nyren O. Aspirin and risk for gastric cancer: a population-based case-control study in Sweden. *Br J Cancer* 2001; **84**: 965–8.
13 Ristimäki A, Honkanen N, Jänkälä H, Sipponen P, Härkönen M. Expression of cyclooxygenase-2 in human gastric carcinoma. *Cancer Res* 1997; **57**: 1276–80.
14 Saukkonen K, Rintahaka J, Sivula A *et al.* Cyclooxygenase-2 and gastric carcinogenesis. *APMIS* 2003; **111**: 915–25.
15 Saukkonen K, Nieminen O, van Rees B *et al.* Expression of cyclooxygenase-2 in dysplasia of the stomach and in intestinal-type gastric adenocarcinoma. *Clin Cancer Res* 2001; **7**: 1923–31.
16 Correa P. *Helicobacter pylori* infection and gastric cancer. *Cancer Epidemiol Biomarkers Prev* 2003; **12**: 238s–41s.
17 McCarthy CJ, Crofford LJ, Greenson J, Scheiman JM. Cyclooxygenase-2 expression in gastric antral mucosa before and after eradication of *Helicobacter pylori* infection. *Am J Gastroenterol* 1999; **94**: 1218–23.
18 Smith MF Jr, Mitchell A, Li G *et al.* Toll-like receptor (TLR) 2 and TLR5, but not TLR4, are required for *Helicobacter pylori*-induced NF-κB activation and chemokine expression by epithelial cells. *J Biol Chem* 2003; **278**: 32 552–60.
19 Chang YJ, Wu MS, Lin JT *et al.* Induction of cyclooxygenase-2 overexpression in human gastric epithelial cells by *Helicobacter pylori* involves TLR2/TLR9 and c-Src-dependent nuclear factor-κB activation. *Mol Pharmacol* 2004; **66**: 1465–77.
20 Chang YJ, Wu MS, Lin JT, Chen CC. *Helicobacter pylori*-induced invasion and angiogenesis of gastric cells is mediated by cyclooxygenase-2 induction through TLR2/TLR9 and promoter regulation. *J Immunol* 2005; **175**: 8242–52.
21 Murakami M, Naraba H, Tanioka T *et al.* Regulation of prostaglandin E_2 biosynthesis by inducible membrane-associated prostaglandin E_2 synthase that acts in concert with cyclooxygenase-2. *J Biol Chem* 2000; **275**: 32783–92.
22 van Rees BP, Sivula A, Thorén S *et al.* Expression of microsomal prostaglandin E synthase-1 in intestinal type gastric adenocarcinoma and in gastric cancer cell lines. *Int J Cancer* 2003; **107**: 551–6.
23 Jang TJ. Expression of proteins related to prostaglandin E_2 biosynthesis is increased in human gastric cancer and during gastric carcinogenesis. *Virchows Arch* 2004; **445**: 564–71.
24 Nardone G, Rocco A, Vaira D *et al.* Expression of COX-2, mPGE-synthase1, MDR-1 (P-gp), and Bcl-X_L: a molecular pathway of *H. pylori*-related gastric carcinogenesis. *J Pathol* 2004; **202**: 305–12.
25 Uefuji K, Ichikura T, Mochizuki H. Cyclooxygenase-2 expression is related to prostaglandin biosynthesis and angiogenesis in human gastric cancer. *Clin Cancer Res* 2000; **6**: 135–8.
26 Al-Marhoon MS, Nunn S, Soames RW. CagA+ *Helicobacter pylori* induces greater levels of prostaglandin E2 than cagA-strains. *Prostaglandins Other Lipid Med* 2004; **73**: 181–9.
27 Hu PJ, Yu J, Zeng ZR *et al.* Chemoprevention of gastric cancer by celecoxib in rats. *Gut* 2004; **53**: 195–200.
28 Nam KT, Hahm KB, Oh SY *et al.* The selective cyclooxygenase-2 inhibitor nimesulide prevents *Helicobacter pylori*-associated gastric cancer development in a mouse model. *Clin Cancer Res* 2004; **10**: 8105–13.
29 Xiao F, Furuta T, Takashima M, Shirai N, Hanai H. Involvement of cyclooxygenase-2 in hyperplastic gastritis induced by *Helicobacter pylori* infection in C57BL/6 mice. *Aliment Pharmacol Ther* 2001; **15**: 875–86.
30 Magari H, Shimizu Y, Inada K *et al.* Inhibitory effects of etodolac, a selective cyclooxygenase-2 inhibitor, on stomach carcinogenesis in *Helicobacter pylori*-infected mongolian gerbils. *Biochem Biophys Res Commun* 2005; **334**: 606–12.
31 Futagami S, Suzuki K, Hiratsuka T *et al.* Celecoxib inhibits Cdx2 expression and prevents gastric cancer in *Helicobacter pylori*-infected mongolian gerbils. *Digestion* 2006; **74**: 187–98.
32 Oshima H, Oshima M, Inaba K, Taketo MM. Hyperplastic gastric tumors induced by activated macrophages in COX-2 /mPGES-1 transgenic mice. *EMBO J* 2004; **23**: 1669–78.
33 Oshima M, Oshima H, Matsunaga A, Taketo MM. Hyperplastic gastric tumors with spasmolytic polypeptide-expressing metaplasia caused by tumor necrosis factor-α-dependent inflammation in cyclooxygenase-2/microsomal prostaglandin E synthase-1 transgenic mice. *Cancer Res* 2005; **65**: 9147–51.
34 Nomura S, Baxter T, Yamaguchi H *et al.* Spasmolytic polypeptide expressing metaplasia to preneoplasia in *H. felis*-infected mice. *Gastroenterology* 2004; **127**: 582–94.
35 Takasu S, Tsukamoto T, Cao X-Y *et al.* Role of cyclooxygenase-2 and microsomal prostaglandin E synthase-1 expression and β-catenin activation in gastric carcinogenesis in *N*-merhyl-*N*-nitrosourea-treated K19-C2mE transgenic mice. *Cancer Sci* 2008; **99**: 2356–64.
36 Taketo MM. Wnt signaling and gastrointestinal tumorigenesis in mouse models. *Oncogene* 2006; **25**: 7522–30.
37 Gregorieff A, Clevers H. Wnt signaling in the intestinal epithelium: from endoderm to cancer. *Genes Dev* 2005; **19**: 877–90.
38 Offerhaus GJ, Giardiello FM, Krush AJ *et al.* The risk of upper gastrointestinal cancer in familial adenomatous polyposis. *Gastroenterology* 1992; **102**: 1980–2.
39 Clements WM, Wang J, Sarnaik A *et al.* β-catenin mutation is a frequent cause of Wnt pathway activation in gastric cancer. *Cancer Res* 2002; **62**: 3503–6.
40 Oshima H, Matsunaga A, Fujimura T, Tsukamoto T, Taketo MM, Oshima M. Carcinogenesis in mouse stomach by simultaneous activation of the Wnt signaling and prostaglandin E_2 pathway. *Gastroenterology* 2006; **131**: 1086–95.
41 Park WS, Oh RR, Park JY *et al.* Frequent somatic mutations of the β-catenin gene in intestinal-type gastric cancer. *Cancer Res* 1999; **59**: 4257–60.

doi: 10.1111/j.1349-7006.2009.01258.x

42 Woo DK, Kim HS, Lee HS, Kang YH, Yang HK, Kim WH. Altered expression and mutation of β-catenin gene in gastric carcinomas and cell lines. *Int J Cancer* 2001; **95**: 108–13.
43 Ebert MPA, Fei G, Kahmann S *et al.* Increased β-catenin mRNA levels and mutational alterations of the *APC* and β-catenin gene are present in intestinal-type gastric cancer. *Carcinogenesis* 2002; **23**: 87–91.
44 Cheng XX, Wang ZC, Chen XY *et al.* Correlation of Wnt-2 expression and β-catenin intracellular accumulation in Chinese gastric cancers: relevance with tumour dissemination. *Cancer Lett* 2005; **223**: 339–47.
45 Kim CJ, Song JH, Cho YG *et al.* Somatic mutations of the β-*TrCP* gene in gastric cancer. *APMIS* 2007; **115**: 127–33.
46 Nojima M, Suzuki H, Toyota M *et al.* Frequent epigenetic inactivation of SFRP genes and constitutive activation of Wnt signaling in gastric cancer. *Oncogene* 2007; **26**: 4699–713.
47 Entius MM, Westerman AM, van Velthuysen ML *et al.* Molecular and phenotypic markers of hamartomatous polyposis syndromes in the gastrointestinal tract. *Hepatogastroenterology* 1999; **46**: 661–6.
48 Howe JR, Bair JL, Sayed MG *et al.* Germline mutations of the gene encoding bone morphogenetic protein receptor 1A in juvenile polyposis. *Nat Genet* 2001; **28**: 184–7.
49 Miyazono K, Maeda S, Imamura T. BMP receptor signaling: transcriptional targets, regulation of signals, and signaling cross-talk. *Cytokine Growth Factor Rev* 2005; **16**: 251–63.
50 Chen D, Zhao M, Mundy GR. Bone morphogenetic proteins. *Growth Factors* 2004; **22**: 233–41.
51 Hardwick JCH, van den Brink GR, Bleuming SA *et al.* Bone morphogenetic protein 2 is expressed by, and acts upon, mature epithelial cells in the colon. *Gastroenterology* 2004; **126**: 111–21.
52 Haramis A-PG, Begthel H, van den Born M *et al.* De novo crypt formation and juvenile polyposis on BMP inhibition in mouse intestine. *Science* 2004; **303**: 1684–6.
53 He XC, Zhang J, Tong W-G *et al.* BMP signaling inhibits intestinal stem cell self-renewal through suppression of Wnt-β-catenin signaling. *Nat Genet* 2004; **36**: 1117–21.
54 Auclair BA, Benoit YD, Rivard N, Mishina Y, Perreault N. Bone morphogenetic protein signaling is essential for terminal differentiation of the intestinal secretory cell lineage. *Gastroenterology* 2007; **133**: 887–96.
55 Chow E, Macrae F. Review of juvenile polyposis syndrome. *J Gastroenterol Hepatol* 2005; **20**: 1634–40.
56 Schreibman IR, Baker M, Amos C, McGarrity TJ. The hamartomatous polyposis syndromes: a clinical and molecular review. *Am J Gastroenterol* 2005; **100**: 476–90.
57 Wen XZ, Miyake S, Akiyama Y, Yuasa Y. BMP-2 modulates the proliferation and differentiation of normal and cancerous gastric cells. *Biochem Biophys Res Commun* 2004; **316**: 100–6.
58 Wen XZ, Akiyama Y, Baylin S, Yuasa Y. Frequent epigenetic silencing of the bone morphogenetic protein 2 gene through methylation in gastric carcinomas. *Oncogene* 2006; **25**: 2666–73.
59 Oshima H, Itadani H, Kotani H, Taketo MM, Oshima M. Induction of prostaglandin E_2 pathway promotes gastric hamartoma development with suppression of bone morphogenetic protein signaling. *Cancer Res* 2009; **69**: 2729–33.
60 Covarrubias DJ, Huprich JE. Best cases from the AFIP. Juvenile polyposis of the stomach. *Radiographics* 2002; **22**: 415–20.
61 Fodde R, Brabletz T. Wnt/β-catenin signaling in cancer stemness and malignant behavior. *Curr Opin Cell Biol* 2007; **19**: 150–8.
62 Brabletz T, Jung A, Hermann K, Günther K, Hohenberger W, Kirchner T. Nuclear overexpression of the oncoprotein β-catenin in colorectal cancer is localized predominantly at the invasion front. *Pathol Res Pract* 1998; **194**: 701–4.
63 Rasola A, Fassetta M, De Bacco F *et al.* A positive feedback loop between hepatocyte growth factor receptor and β-catenin sustains colorectal cancer cell invasive growth. *Oncogene* 2006; **26**: 1078–87.
64 Yang L, Lin C, Liu ZR. P68 RNA helicase mediates PDGF-induced epithelial mesenchymal transition by displacing Axin from β-catenin. *Cell* 2006; **127**: 139–55.
65 Oguma K, Oshima H, Aoki M *et al.* Activated macrophages promote Wnt signaling through tumor necrosis factor-α in gastric tumor cell. *EMBO J* 2008; **27**: 1671–81.

Carcinogenesis vol.29 no.2 pp.440–447, 2008
doi:10.1093/carcin/bgm274
Advance Access publication January 3, 2008

Platelet-type 12-lipoxygenase accelerates tumor promotion of mouse epidermal cells through enhancement of cloning efficiency

Ying-Shi Piao[1,2,3], Yu-Chen Du[1,2], Hiroko Oshima[1], Jing-Chun Jin[4], Masaaki Nomura[5], Tanihiro Yoshimoto[2] and Masanobu Oshima[1,*]

[1]Division of Genetics, Cancer Research Institute, [2]Department of Pharmacology, Graduate School of Medicine, Kanazawa University, Kanazawa 920-0934, Japan, [3]Department of Physiology and Pathophysiology, [4]Department of Hematology, Medical College, Yanbian University, Yanji 133000, Jilin, China and [5]Department of Clinical Pharmacology, Faculty of Pharmaceutical Sciences, Hokuriku University, Kanazawa 920-1181, Japan

*To whom correspondence should be addressed. Tel: +81 76 265 2721; Fax: +81 76 234 4519; Email: oshimam@kenroku.kanazawa-u.ac.jp

Accumulating evidence suggests that platelet-type 12-lipoxygenase (*p*12-LOX) plays an important role in tumor development. However, how *p*12-LOX contributes to tumorigenesis is still not understood. The role of *p*12-LOX was therefore examined in tumor promotion using mouse epidermal JB6 P+ cells that are sensitive to 12-*O*-tetradecanoylphorbol-13-acetate-induced transformation. The expression of *p*12-LOX was significantly higher in JB6 P+ cells than in JB6 P− cells that were resistant to transformation, and its expression was further increased by tumor necrosis factor (TNF)-α. Importantly, the inhibition of *p*12-LOX in JB6 P+ cells by baicalein, a specific inhibitor or small interfering RNA significantly suppressed TPA-induced transformation. Moreover, treatment with 12(*S*)-hydroxyeicosatetraenoic acid (HETE), a metabolite of *p*12-LOX, enhanced TPA-induced neoplastic transformation either in the presence or absence of baicalein. These results indicate that *p*12-LOX is required for tumor promotion of epidermal cells and that 12(*S*)-HETE functions as a rate-limiting factor. Notably, treatment with baicalein significantly suppressed the proliferation of JB6 P+ cells when cells were seeded at a low density in a culture plate. Moreover, the cloning efficiency of JB6 P+ cells was dramatically decreased by inhibition of *p*12-LOX. In contrast, baicalein treatment did not affect the cloning efficiency of most malignant cancer cells. These results indicate that *p*12-LOX is induced by the inflammatory cytokine TNF-α in the early stage of tumorigenesis, and is required for tumor promotion through enhancing efficient proliferation of a small number of initiated cells. The present results suggest that the *p*12-LOX pathway may be an effective target of chemoprevention for skin carcinogenesis.

Introduction

The cyclooxygenase (COX) and lipoxygenase (LOX) are two important enzyme classes that metabolize polyunsaturated fatty acids and play important roles in tumorigenesis (1). COX-2, one of the COX isoenzymes, plays a variety of pathological roles including cancer development (2). Previous studies have demonstrated that the induction of COX-2 is responsible for intestinal tumorigenesis (3) and that prostaglandin (PG)E_2, one of downstream products of COX-2, is required for carcinogenesis in the stomach through cross-talk with activated Wnt signaling (4,5).

Abbreviations: COX, cyclooxygenase; GAPDH, glyceraldehydes-3-phosphate dehydrogenase; HETE, hydroxyeicosatetraenoic acid; LOX, lipoxygenase; MTT, 3-(4,5-dimethylthiazol-2-yl)-2,5-dimethyltetrazolium bromide; NDGA, nordihydroguaiaretic acid; *p*12-LOX, platelet-type 12- lipoxygenase; PG, prostaglandin; RT–PCR, reverse transcription–polymerase chain reaction; siRNA, small interfering RNA; TNF-α, tumor necrosis factor-α; TPA, 12-*O*-tetradecanoylphorbol-13-acetate.

Among the LOX family members, it has been suggested that platelet-type 12-lipoxygenase (*p*12-LOX) plays an important role in tumorigenesis (6,7). The expression of *p*12-LOX is absent or at a basal level in the normal tissues (6,8). However, the induction of *p*12-LOX is widely found in human cancer tissues that develop in the colon (9), prostate (10,11), stomach (12) and skin (13). In animal models, the *p*12-LOX expression is also found in xenografts of melanoma (9) and in skin tumors developed by an initiation/promotion protocol (14). Moreover, it has been shown that *p*12-LOX expression is associated with the advanced stages of human prostate cancer and its levels increase in metastasized tumors in a mouse model (10,11). These analyses suggest that *p*12-LOX contributes to development and progression of various types of cancers.

The treatment of cancer cells with baicalein, a *p*12-LOX inhibitor, has also been shown to result in the induction of apoptosis and inhibition of tumor xenograft growth in immunodeficient mice (13, 15–17). Consistently, the forced expression of the *p*12-LOX gene or stimulation with 12(*S*)-hydroxyeicosatetraenoic acid (HETE), a metabolite of *p*12-LOX, has been shown to induce cell proliferation and survival (16,18,19). Moreover, it has been reported that *p*12-LOX induces cell spreading, integrin-dependent cell survival (19,20) and angiogenesis through the induction of vascular endothelial growth factor expression (21,22). Accordingly, it is conceivable that the *p*12-LOX pathway also contributes to tumor progression through the acceleration of cell survival, migration and angiogenesis.

Genetic experiments have indicated that *p*12-LOX plays an important role in skin tumorigenesis. In the initiation/promotion skin carcinogenesis model, multiplicity and incidence of squamous cell carcinoma are suppressed significantly by the disruption of the *p*12-LOX gene (23). Accordingly, it is possible that *p*12-LOX is important for tumor promotion of the initiated cells during skin carcinogenesis. To assess this possibility, we have investigated the role of *p*12-LOX and 12(*S*)-HETE in promotion of epidermal cell transformation using mouse JB6 P+ cell line. The cells of this line are transformed by stimulation with tumor promoters such as TPA or tumor necrosis factor (TNF)-α and, therefore, are useful to examine the mechanisms involved in the promotion of epidermal cell transformation (24,25). Clonal variant JB6 P− cells are resistant to tumor promoter-induced transformation. As a result, we therefore used JB6 P− cells, in addition to P+ cells, to examine the role of *p*12-LOX in the transformation process.

We demonstrate here that expression of *p*12-LOX is increased significantly in JB6 P+ cells but not in JB6 P− cells. Moreover, inhibition of *p*12-LOX of JB6 P+ cells suppresses colony formation in soft agar, whereas treatment with 12(*S*)-HETE accelerates it. In addition, we show that the *p*12-LOX pathway is responsible for proliferation from a single cell or a small number of cells. These results suggest that *p*12-LOX contributes to tumor promotion through the acceleration of initiated cell proliferation and that lack of *p*12-LOX is thus considered to be one of the causes for the resistance of JB6 P− cells against tumor promoter-induced transformation.

Materials and methods

Reverse transcription–polymerase chain reaction analysis

RNA samples were prepared from cultured cells or mouse tissue samples using the ISOGEN solution (Nippongene, Tokyo, Japan). Mouse gastric tumors and intestinal polyps were obtained from *K19-Wnt1/C2mE* mice (6) and *Apc*^{1716} mice (26), respectively. Control tissues were obtained from normal tissues of the same mice or wild-type mice. Extracted RNA was reverse transcribed and amplified by PCR with the following primer set: *p*12-LOX (F-5′-GCGGTCTTCGAATTGAACTT-3′ and R-5′-CAGGAACAGTGTTGGAGCTG-3′); epidermal-type 12-LOX (F-5′-CAGGAGCTGGAGAACAGAAGG-3′ and R-5′-GAACTGGTACCCAAAGAGAGCATC-3′); leukocyte-type 12-LOX

(F-5′-GGCTCCAACAACGAGGTCTA-3′ and R-5′-AGTTCCTCCTCCCTGTGGTT-3′); 5-LOX (F-5′-AATGGAGGTGGTGAGCATCTA-3′ and R-5′-TCCTTCACTGGCTTCTCAATG-3′); 8-LOX (F-5′-CGAAATGCAGGGTGAGAGTA-3′ and R-5′-TCCTGCAGTGTAGGGTGATG-3′). Animal experiments were carried out according to the protocol approved by the Committee on Animal Experimentation on Kanazawa University.

Cell culture and soft agar colony formation assay

JB6 P+ (Cl 41-5a) and JB6 P− (Cl 30-7b) cells were obtained from the American Type Culture Collection (Manassas, VA). The cells were cultured in modified Eagle's medium supplemented with 5% fetal bovine serum and incubated in a 5% CO_2 at 37°C. For the soft agar colony formation assay, JB6 P+ and JB6 P− cells were exposed to TPA (Calbiochem, San Diego, CA) at 10 ng/ml in 1 ml of basal medium eagle (Invitrogen, Grand Island, NY) with 10% fetal bovine serum and 0.33% agar and then seeded in a six-well plate (10^4 cells per well). Soft agar cultures were maintained in a 5% CO_2 incubator at 37°C for 14 days and stained with Giemsa stain solution (Wako, Osaka, Japan) and the number of colonies was scored using a stereomicroscope and Image J software program (National Institutes of Health). A non-selective LOX inhibitor nordihydroguaiaretic acid (NDGA), a selective 12-LOX inhibitor baicalein (Tocris Biosciences, Ellisville, MI) or a selective 5-LOX inhibitor AA-861 (Sigma, St Louis, MO) was added to the agar containing medium at 5 μM (NDGA and baicalein) or 10 μM (AA-861) to test their inhibitory effect on anchorage-independent transformation. To examine the effect of 12(*S*)-HETE, cells were pre-treated with 12(*S*)-HETE (Cayman Chemical, Ann Arbor, MI) at 0.1 μM or 1 μM for 1 day prior to stimulation with TPA and were plated as described above for the soft agar colony formation assay. All soft agar colony formation assays were repeated three times, and the mean colony numbers and standard deviation were calculated.

Subcutaneous transplantation of tumor cells to mice

JB6 P+ cells were stimulated with TPA at 10 ng/ml for 12 h and inoculated subcutaneously at 1.0×10^6 cells per site to three sites per mouse for four mice each for drug-treated and no-treated group (Balb/c-nu/nu: Charles River Laboratories Japan, Tokyo, Japan). At 5 days after inoculation, 50 μl of TPA (10 ng/ml in phosphate-buffered saline) was injected subcutaneously, into the inoculation site. After palpable tumors developed, baicalein was administered at 20 mg/kg/day in 0.5% methylcellulose (Wako) *per os*, and treatment was continued for 14 days. In another dosing experiment, baicalein treatment started from day 7 after cell inoculation and the treatment was continued until 1 week after palpable tumors developed in the control mice. The dosing protocol has been reported to inhibit *p*12-LOX activity *in vivo* (27). The tumor size was measured every 2 days during drug treatment using six developed tumors for each experiment and the mean tumor volume and standard error were calculated.

BrdU labeling analysis

Mice were injected intra-peritoneally with 100 μl of BrdU solution (BD Pharmingen, San Diego, CA) at 1 h before euthanasia. The tumor tissues were fixed in 4% paraformaldehyde, embedded and sectioned at 4-μm thickness. These sections were stained with anti-BrdU antibody (BD Pharmingen). The immunostaining analysis was repeated three times.

Small interfering RNA transfection

The target sequence of three small interfering RNAs (siRNAs) against *p*12-LOX were as follows: A, sense: GGGUGCAGGGAGAGGGAAUTT, antisense: AUUCCCUCUCCCUGCACCCTT; B, sense: GGAUGGAAUUCCAGCUAAUTT, antisense: AUUAGCUGGAAUUCCAUCCTT and C, sense: CAUCUCAGAUGGAGGAAUATT, antisense: UAUUCCUCCAUCUGAGAUGTT. We confirmed the siRNA sequences to be specific for mouse *p*12-LOX by GenBank database search. There is no transcript in the database that has >80% homology with siRNA sequences except for *p*12-LOX. These three siRNAs (A, B and C) were mixed and transfected into JB6 P+ cells at 50 nM using siFECTOR (B-Bridge, Sunnyvale, CA) prior to TPA stimulation. A decrease of *p*12-LOX mRNA by siRNA transfection was confirmed by RT–PCR and immunoblotting analysis.

Immunoblotting analysis

Cells were collected in buffer and sonicated. After centrifugation at 20 000*g*, 20 μg of the supernatant was separated in a 10% sodium dodecyl sulfate–polyacrylamide gel. Antibody for 12-LOX (Santa Cruz Biotechnology, Carlsbad, CA) was used as the primary antibody. The enhanced chemiluminescence detection system (Amersham Biosciences, Buckinghamshire, UK) was used to detect the specific signals.

NF-κB activation assay

JB6 P+ and JB6 P− cells were stimulated with TNF-α (Calbiochem) at 10 ng/ml in the presence or absence of baicalein (Tocris Biosciences) at 5 μM, and the nuclear extract of these cells was prepared using NE-PER Nuclear and Cytoplasmic Extraction Reagents (PIERCE, Rockford, IL). Activity of NF-κB was measured using NF-κB p65 Transcription Factor Assay Kit (Active Motif, Carlsbad, CA).

Cell proliferation assay

The cell proliferation rate was determined using an 3-(4,5-dimethylthiazol-2-yl)-2,5-diphenyltetrazolium bromide (MTT) assay kit (Nacalai Tesque, Kyoto, Japan) according to the manufacturer's protocol. Briefly, 10^2 or 10^3 cells were plated to each well of a 96-well microplate and cultured overnight, and the cells of the drug-treated group were treated with NDGA (5 μM) or baicalein (5 μM). Following the drug exposure period (4 or 6 days), 10 μl of MTT (5 mg/ml in phosphate-buffered saline) was added to each well and then the cells were cultured further for 4 h. The formazan crystals that were produced by these cultures were solubilized using 100 μl of isopropyl alcohol containing hydrochloric acid at 40 mM, and the absorbance at 570 nm was measured. All experiments were repeated three times and the mean relative MTT assay results to the no-drug control groups were then calculated and presented.

Cloning efficiency assay

JB6 P+ cells, two gastric cancer cells: AGS (American Type Culture Collection) and Kato-III (Cell Resource Center for Biomedical Research, Tohoku University, Japan) and three colon cancer cells: HCT-116 (American Type Culture Collection), DLD-1 and SW480 (Cell Resource Center for Biomedical Research) were used for the cloning efficiency experiments. The gastrointestinal cancer cells were maintained in Roswell Park Memorial Institute (AGS, Kato-III and DLD-1) or Dulbecco's modified Eagle's medium (SW480 and HCT-116) supplemented with 10% fetal bovine serum and cultured in a 5% CO_2 incubator at 37°C. The cells were suspended in the medium at 10 cells/ml, and 100 μl was dispensed to each well of 96-well microplate to expect plating a single cell in each well. To examine the effect of *p*12-LOX on cloning efficiency, siRNA for *p*12-LOX was transfected prior to TPA stimulation or baicalein was added to the medium at 5 μM. After culture for 14 days, all wells were stained with Giemsa stain solution (Wako). All experiments were repeated three times and the cloning efficiency was calculated by dividing the number of wells containing proliferating cells with the total number of cell-plated wells.

Statistical analysis

The statistical significance of differences was determined by Student's *t*-test. Differences with a value of $P < 0.05$ were considered to be significant.

Results

Increased expression of p12-LOX in promotion-sensitive JB6 P+ cells

The expression level of *p*12-LOX was first examined by RT–PCR in the promotion-sensitive JB6 P+ cells as well as in promotion-resistant JB6 P− cells. The level of *p*12-LOX mRNA in the JB6 P+ cells was significantly higher than that in the JB6 P− cells (Figure 1A). Stimulation with TPA at 10 ng/ml increased the *p*12-LOX expression level in JB6 P− cells, although its highest level at 12 h was lower than that of the basal level of JB6 P+ cells. In contrast, *p*12-LOX in the TPA-stimulated JB6 P+ cells was increased only slightly possibly caused by constitutive elevation of the basal level. No significant differences were observed in either the expression of other LOX family members, such as epidermal-type 12-LOX, leukocyte-type 12-LOX, 5-LOX and 8-LOX between JB6 P+ cells and JB6 P− cells (Figure 1A).

Suppression of anchorage-independent transformation of JB6 P+ cells by inhibition of p12-LOX

TPA treatment induced soft agar colony formation of JB6 P+ cells but not of JB6 P− cells that are a resistant line to tumor promoter-induced transformation (Figure 1B). When JB6 P+ cells were treated with a non-specific LOX inhibitor NDGA at 5 μM, the number of soft agar colonies decreased significantly by 88%. Moreover, treatment with baicalein, a *p*12-LOX specific inhibitor, at 5 μM also suppressed colony formation in soft agar of JB6 P+ cells by 81% (Figure 1B and C). It has been suggested that 5-LOX is also procarcinogenic lipoxygenase among the LOX family members (1,6). However, treatment with AA-861, a 5-LOX specific inhibitor, at 10 μM did not reduce the number of soft agar colonies (Figure 1B and C). These results indicate that *p*12-LOX but not 5-LOX plays an important role in the neoplastic transformation of JB6 P+ cells.

Baicalein has been reported to be a potent inhibitor of both reticulocyte 15-LOX and *p*12-LOX (28). Therefore, the effects of

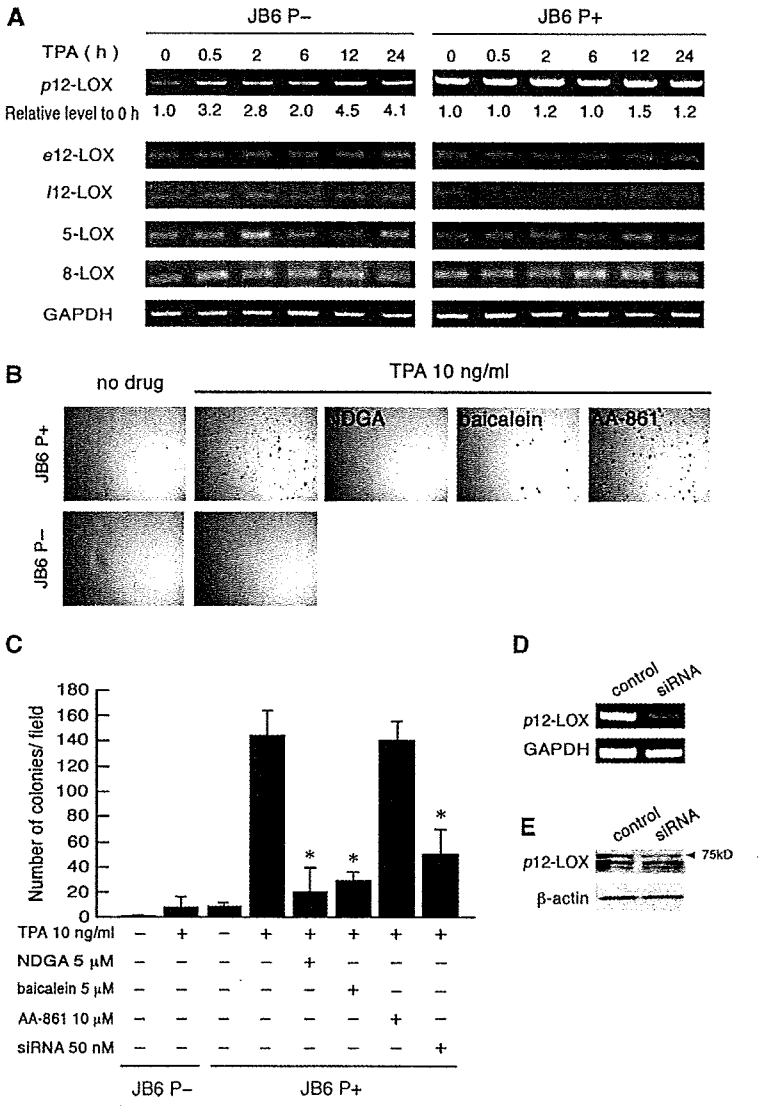

Fig. 1. The inhibition of *p*12-LOX in transformation-sensitive JB6 P+ cells suppresses colony formation in soft agar. (**A**) Representative RT–PCR results for the *p*12-LOX, epidermal type 12-LOX (*e*12-LOX), leukocyte type 12-LOX (*l*12-LOX), 5-LOX and 8-LOX are shown. The expression of *p*12-LOX is elevated in transformation-sensitive JB6 P+ cells, whereas it remains at the basal level in transformation-resistant JB6 P– cells. The expression of other LOX members is at the same level between JB6 P+ and JB6 P– cells. Glyceraldehyde-3-phosphate dehydrogenase (GAPDH) was used as internal control. JB6 P+ and P– cells were stimulated with TPA (10 ng/ml) for 24 h, and the mRNA levels were examined by RT–PCR chronologically at the respective time points indicated. Relative band intensity of *p*12-LOX to the level at 0 h is indicated. (**B**) Representative photographs of soft agar cultures of JB6 P+ (top) and JB6 P– (bottom) cells are shown (Giemsa staining). TPA treatment (10 ng/ml) induced soft agar colony formation in JB6 P+ cells (top, second panel from left) but not in JB6 P– cells (bottom, second panel from left). Cells were treated with NDGA (5 μM), baicalein (5 μM) or AA-861 (10 μM) in the presence of TPA (right three panels). Note that treatment with a non-selective LOX inhibitor, NDGA, and a selective *p*12-LOX inhibitor, baicalein, resulted in significant suppression of soft agar colony formation, whereas the 5-LOX inhibitor, AA-861, treatment did not. (**C**) The mean number of colonies per field (mean ± SD) is shown. Treatments of the cells (drug treatment or siRNA transfection) are indicated below the histogram. $^{*}P < 0.05$ versus no-drug control of TPA-stimulated JB6 P+ cells. (**D**) Representative RT–PCR for *p*12-LOX in the siRNA-transfected JB6 P+ cells is shown. GAPHD was used as an internal control. (**E**) Immunoblotting for *p*12-LOX in the siRNA-transfected JB6 P+ cells is shown. β-Actin was used as an internal control.

*p*12-LOX inhibition on soft agar colony formation were examined using a specific siRNA. Transient transfection of siRNA against the *p*12-LOX gene reduced the mRNA level in comparison with that of control cells (Figure 1D). We also confirmed the protein level of *p*12-LOX to have decreased in the siRNA-transfected JB6 cells (Figure 1E). Importantly, the inhibition of *p*12-LOX in JB6 P+ cells by siRNA transfection caused a significant suppression of TPA-induced neoplastic transformation by 61% compared with that in the control cells (Figure 1C). Therefore, the siRNA experiments confirmed the role of *p*12-LOX in promotion step of JB6 P+ cell transformation.

p12-LOX-independent growth of TPA-induced JB6 P+ tumors in nude mice

We examined the possibility that *p*12-LOX is required for the *in vivo* growth of tumor tissues consisting of JB6 P+ cells. TPA-stimulated JB6 P+ cells formed palpable tumors in nude mice at 22 days after subcutaneous inoculation (Figure 2A). In contrast to the anchorage-independent transformation assays, treatment of the mice with baicalein at 20 mg/kg/day from day 26 to 40 (14 days) did not suppress tumor growth (Figure 2A and B). There was no significant difference

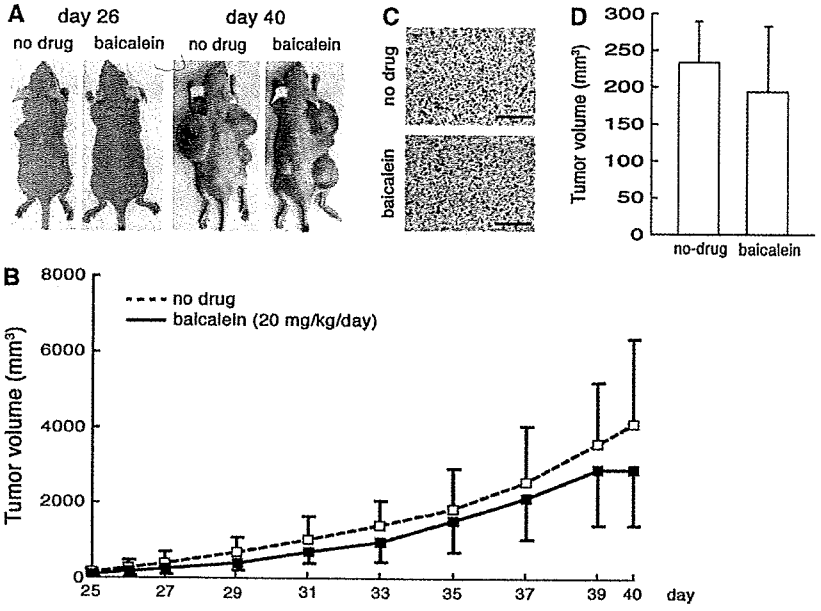

Fig. 2. The inhibition of *p*12-LOX does not affect the tumor growth of JB6 P+ cells *in vivo*. (**A**) Photographs of TPA-stimulated JB6 P+ tumors developed in nude mice before (left) and after (right) baicalein treatment (20 mg/kg/day) at 26 and 40 days after the inoculation of tumor cells, respectively. (**B**) The tumor volume changes from day 25 to day 40 (mean ± SE) are shown. Solid lines indicate baicalein-treated mouse tumors, whereas dashed lines show no-drug control mouse tumors. (**C**) Representative photograph of BrdU incorporation (1 h) in the baicalein-treated tumor (right) and no-drug control tumor (left). Bars indicate 100 μm. Note that BrdU incorporation has increased in both baicalein-treated and baicalein-untreated mouse tumors. (**D**) Tumor volume at 1 week after palpable tumor developed in the baicalein-treated mice (from day 7) and no-treated mice (mean ± SE) is shown.

in the BrdU incorporation in tumor cells between baicalein-treated and non-treated mouse tumors (Figure 2C). Moreover, tumor development was not suppressed when the baicalein treatment started from day 7 after tumor cell inoculation (Figure 2D). These observations suggest that *p*12-LOX is less important for the JB6 tumor growth *in vivo* which develops from 10^6 inoculated cells. Rather, *p*12-LOX appeared to play an important role in the proliferation from a single JB6 cell (see below).

Acceleration TPA-induced transformation of JB6 P+ cells by 12(S)-HETE treatment

We next examined the role of 12(*S*)-HETE, a metabolite of *p*12-LOX, in tumor promotion. JB6 P+ cells were pre-treated with 12(*S*)-HETE and the TPA-induced soft agar colony formation in the presence or absence of baicalein was examined. Notably, the treatment of JB6 P+ cells with 12(*S*)-HETE reversed the inhibitory effects of baicalein on TPA-induced colony formation in a dose-dependent manner (Figure 3A and B), thus indicating that 12(*S*)-HETE is responsible for tumor promotion of JB6 P+ cells.

Importantly, even in the absence of baicalein, the number of TPA-induced soft agar colonies of JB6 P+ cells was significantly increased by treatment with 12(*S*)-HETE in a dose-dependent manner (Figure 3A and B). In contrast, 12(*S*)-HETE treatment alone did not induce the soft agar colony formation of the TPA-untreated JB6 P+ cells. These results, taken together, indicate that 12(*S*)-HETE is a rate-limiting factor for the promotion of JB6 P+ cell transformation, although stimulation by a tumor promoter, such as TPA, is still necessary for such promotion.

Induction of p12-LOX by TNF-α stimulation

JB6 P+ cells are also transformed by TNF-α stimulation, and TNF-α-activated NF-κB is important for neoplastic transformation of JB6 P+ cells (29,30). Stimulation with TPA, acting through the mitogen-activated protein kinase pathway, activates AP-1 and subsequently NF-κB in JB6 P+ cells (31). Therefore, we examined the possibility that *p*12-LOX is involved in activation of NF-κB in the TNF-α-stimulated JB6 P+ cells. Consistent with the findings of a previous report, the treatment of JB6 P+ cells with TNF-α significantly increased the NF-κB activity (Figure 4A). Notably, the treatment of the cells with baicalein did not affect the NF-κB activity in the TNF-α-stimulated cells, indicating that the *p*12-LOX pathway is not required for the activation of NF-κB. Although NF-κB was activated by TNF-α in JB6 P− cells, the level was significantly lower than that in JP6 P+ cells (Figure 4A). We also confirmed that the TNF-α-induced NF-κB activation in JB6 P− cells was not suppressed by the baicalein treatment. In contrast, stimulation with TNF-α induced the *p*12-LOX expression both in JB6 P+ and JB6 P− cells (Figure 4B), thus suggesting that *p*12-LOX is induced by inflammatory responses through the TNF-α/NF-κB pathway.

Suppression of cell proliferation by inhibition of p12-LOX

It has been shown that treatment with baicalein at 20–50 μM induces apoptosis and suppresses proliferation in several types of cancer cells (13,15–17). Therefore, the MTT assay was used to determine whether the proliferation of JB6 P+ cells is suppressed by baicalein at 5 μM, the same concentration used in this study. When 10^3 cells were plated in each well of a 96-well microplate, JB6 P+ cells showed approximately 20% decreased proliferation compared with that of the control cells both at day 4 and day 6 (Figure 5). Treatment with NDGA at 5 μM also yielded a similar suppression of proliferation.

Importantly, however, the proliferation of JB6 P+ cells was suppressed more significantly by baicalein or NDGA when 10^2 cells were plated in each well of a 96-well microplate (Figure 5). The number of drug-treated cells decreased by 90% of that of control cells at 6 days; the cells appeared to stop proliferation and they did not reach confluence after continuous culture for several days (data not shown). These results suggest that *p*12-LOX is therefore essential for the proliferation of JB6 P+ cells when cells were plated at a low density. This is consistent with the results of the *in vivo* experiments (Figure 2C) showing that baicalein treatment did not affect cell proliferation in the established tumors, where the cell density was very high.

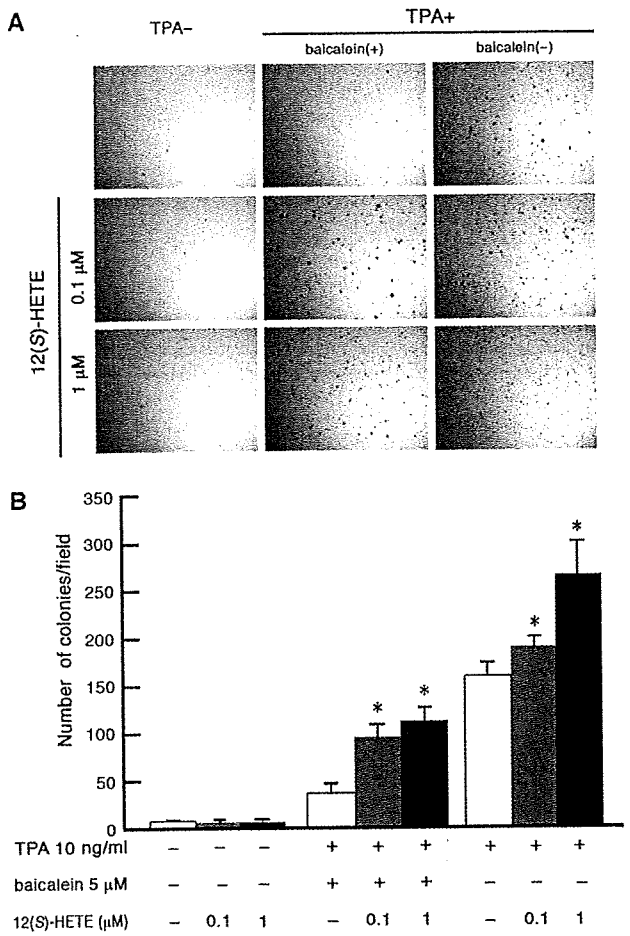

Fig. 3. Treatment with 12(*S*)-HETE enhances TPA-induced neoplastic transformation of JB6 P+ cells. (**A**) Representative photographs of soft agar cultures are shown (Giemsa staining). TPA-negative control cells (left). TPA-stimulated and baicalein-treated cells (center) and TPA-stimulated but baicalein-untreated cells (right). The cells were pre-treated with 12(*S*)-HETE at 0.1 μM (middle panels) and 1 μM (bottom panels). Note that treatment with 12(*S*)-HETE restored soft agar colony formation of baicalein-treated JB6 P+ cells (center panels). The number of colonies increased by 12(*S*)-HETE even in the baicalein-untreated JB6 P+ cells (right panels). (**B**) The mean number of colonies per field is shown (mean ± SD). Treatments of the cells are indicated below the histogram. $^{*}P < 0.05$ versus 12(*S*)-HETE-untreated control of each group.

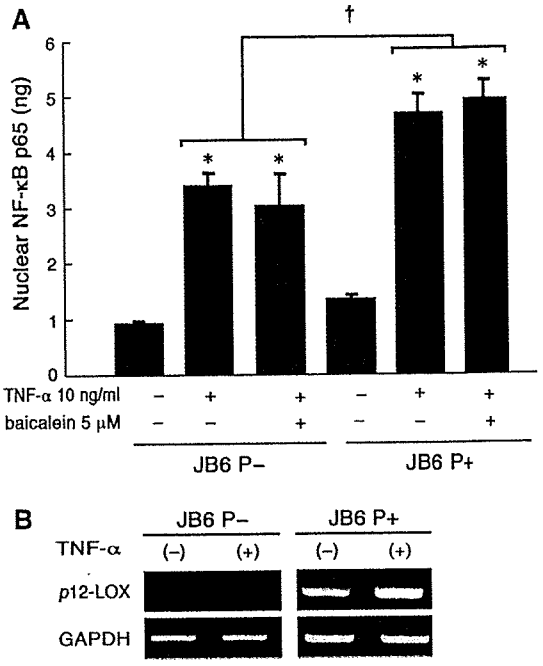

Fig. 4. *p*12-LOX pathway is not required for TNF-α-induced NF-κB activation, but is induced by TNF-α stimulation. (**A**) Relative NF-κB activity to the untreated JB6 P– level is shown (mean ± SD). Treatments of the cells are indicated below the histogram. $^{*}P < 0.05$ versus TNF-α-untreated level of JB6 P– and JB6 P+ cells, respectively. $\dagger P < 0.05$. (**B**) Representative RT–PCR results for *p*12-LOX in the TNF-α-stimulated JB6 cells are shown. The expression of *p*12-LOX is induced both in JB6 P+ and P– cells by TNF-α stimulation. GAPHD was used as internal control.

Decrease of cloning efficiency of JB6 P+ cells by inhibition of p12-LOX

These results prompted us to examine the possibility that *p*12-LOX is required for the proliferation from a solitary single cell. Such ability of proliferation from a single cell is one of the important factors that is required for tumorigenesis. The cloning efficiency of TPA-untreated or TPA-treated JB6 P+ cells was 54% and 44%, respectively (Figure 6B), indicating that the cloning efficiency was independent from TPA treatment. Notably, the transfection of siRNA for *p*12-LOX suppressed the cloning efficiency significantly to 41% and 31% in the TPA-untreated and TPA-treated JB6 P+ cells, respectively (Figure 6A and B). More importantly, baicalein treatment dramatically reduced the cloning efficiency to 3% and 5% in the TPA-untreated and TPA-treated cells, respectively. These results indicate that *p*12-LOX is essential for the clonal proliferation from a solitary JB6 P+ cell, which should be important for the tumor promotion process. Although the suppression of cloning efficiency was more effective after baicalein treatment than that after siRNA transfection, this difference may be attributable to the transfection efficiency of siRNA.

p12-LOX-independent clonal proliferation of malignant cancer cells

To investigate whether *p*12-LOX is required for the tumor promotion step in other tissues, the expression of *p*12-LOX in gastric tumors of *K19-Wnt1/C2mE* mice (5) as well as intestinal polyps of *Apc*^{1716} mice was examined (26). Interestingly, the *p*12-LOX expression was significantly induced in both gastric and intestinal tumor tissues (Figure 6C), suggesting the role of *p*12-LOX in tumorigenesis also in the gastrointestinal tract. Therefore, the cloning efficiency of gastric cancer cells (AGS and Kato-III) and colon cancer cells (DLD-1, SW480 and HCT-116) was examined. The treatment with baicalein at 5 μM significantly decreased the cloning efficiency of SW480 cells, although the colonies still formed in 44% of the plate wells (Figure 6D). The cloning efficiencies in other cell lines did not show significant decrease by the inhibition of *p*12-LOX. Accordingly, it is possible that progressing cancer cells acquire the ability for *p*12-LOX-independent proliferation from a solitary cell, unlike JB6 P+ cells.

Discussion

Accumulating evidence indicates that expression of *p*12-LOX is induced in several types of cancer tissues, whereas its expression is absent or weak in the normal tissues (6). Moreover, *p*12-LOX expression increases in the advanced stage of cancer tissues, and the *p*12-LOX pathway is involved in the suppression of apoptosis, induction of cell survival and angiogenesis (10,15,19,21). These results suggest that the *p*12-LOX pathway plays a role in tumor development, progression and metastasis. In addition to these results, the present study

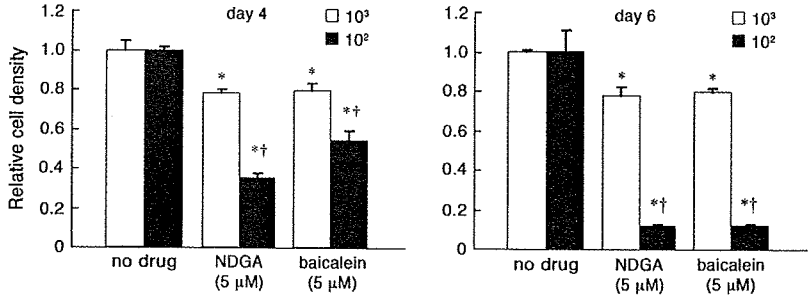

Fig. 5. Inhibition of *p*12-LOX significantly suppresses JB6 P+ cell proliferation when cells are plated at a low density. Relative cell densities to no-drug control at day 4 (left) and day 6 (right) after plating are shown (MTT assay, mean ± SD). Open bars indicate relative cell density in the wells plated with 10^3 cells, whereas black bars indicate 10^2 cells. Note that treatment with NDGA (5 μM) and baicalein (5 μM) suppressed proliferation significantly in the wells plated with 10^2 cells compared with that with 10^3 cells. $^*P < 0.05$ versus no-drug control of the same cell number group; $\dagger P < 0.05$ versus 10^3 cell-plated well of the same drug group.

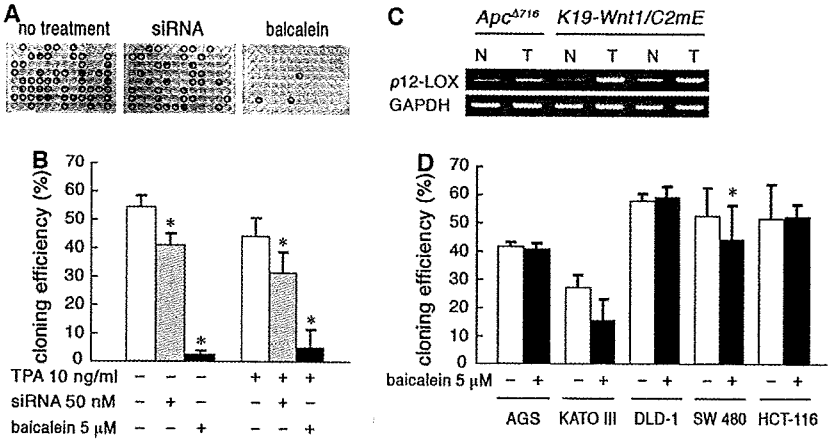

Fig. 6. Inhibition of *p*12-LOX suppresses the cloning efficiency of JB6 P+ cells. (**A**) Representative photographs of a microplate at 14 days after plating with no-drug control, siRNA-transfected and baicalein-treated cells (left to right) in which a single cell was seeded in each well (Giemsa staining). The wells containing proliferating cells are indicated with a circle. Note that treatment with baicalein (5 μM) dramatically suppressed the cloning efficiency. (**B**) The cloning efficiency of JB6 P+ cells is indicated as histogram (mean ± SD). Treatments of the cells are indicated below the histogram. $^*P < 0.05$ versus baicalein-untreated control of each group. (**C**) Expression of *p*12-LOX is induced in gastric and intestinal tumors developed in *K19-Wnt1/C2mE* mice and $Apc^{\Delta 716}$ mice, respectively. Representative RT–PCR results are shown. T indicates tumor, whereas N indicates adjacent normal tissue. GAPHD was used as internal control. (**D**) The cloning efficiencies of gastric and colon cancer cells are indicated as histogram (mean ± SD). Treatments of the cells are indicated below the histogram. $^*P < 0.05$ versus baicalein-untreated control of each group.

demonstrated, by pharmacological and genetic experiments, that *p*12-LOX pathway is required for tumor promotion in mouse epidermal cell transformation. This is consistent with a previous report that disruption of the *p*12-LOX gene in mice suppresses the development of squamous cell carcinoma caused by an initiation/promotion protocol (23). Moreover, the present study has shown that treatment with 12(*S*)-HETE, a metabolite of *p*12-LOX, further increases the number of soft agar colonies in TPA-treated JB6 P+ cells. Accordingly, it is possible that formation of 12(*S*)-HETE functions as a rate-limiting factor for tumor promotion in epidermal cell transformation. This suggests that the induction level of *p*12-LOX may be positively correlated with the efficiency of tumor promotion.

It has been shown that baicalein, a *p*12-LOX inhibitor, induces apoptosis in several types of cancer cells (13,15–17). However, baicalein treatment at the concentration used in this study (5 μM) showed only mild suppressive effect on cell proliferation when 10^3 JB6 P+ cells were plated in the microplate well. When the number of plating cells was reduced to 10^2 cells, however, baicalein treatment at 5 μM significantly suppressed proliferation. Moreover, the cloning efficiency of JB6 P+ cells was suppressed dramatically by the same concentration of baicalein. These results collectively indicate that 12(*S*)-HETE is required for the proliferation of small number of cells or a single cell. In the promotion step of tumorigenesis, the original 'initiated' single cell or a small number of promoted cells need to proliferate to form cluster of tumor cells. Accordingly, it is possible that the *p*12-LOX/12(*S*)-HETE pathway plays a key role in clonal proliferation of initiated cells during the promotion step. In contrast, the cloning efficiency of malignant gastric and colon cancer cells was not affected by inhibition of *p*12-LOX. It is possible that tumor cells derived from progressed cancer tissues have already acquired an ability of 12(*S*)-HETE-independent proliferation from a single cell.

These experiments showed that the expression of *p*12-LOX is induced in epidermal cells by stimulation with TNF-α, suggesting that an inflammatory host response induces *p*12-LOX expression through TNF-α/NF-κB pathway. It has been shown that TPA stimulation also activates NF-κB in JB6 P+ cells (31), which is required for transformation (29,30). It has been established that inflammation plays an important role in cancer development (32). Genetic studies have demonstrated that the activation of the TNF-α/NF-κB pathway is required for tumor development in the mouse colon and liver through the

suppression of apoptosis in tumor cells and the induction of growth factors from stromal cells (33,34). Importantly, the expression of *p*12-LOX is induced not only in epidermal tumor cells but also in gastrointestinal tumors where an inflammatory response is associated (4,5). Accordingly, it is possible that *p*12-LOX is one of the tumor-promoting factors induced by inflammatory responses through the TNF-α/NF-κB pathway in various types of tumors. It has been reported that AP-1 and NF-κB play a critical role in transformation of JB6 P+ cells, and activity of these factors is downregulated in JB6 P− cells (30,31). Our results indicate that the deficiency of *p*12-LOX in JB6 P− cells contributes to a resistant phenotype to tumor promoter-induced transformation. Reactive oxygen species also stimulate the neoplastic transformation of JB6 cells by activating AP-1 and NF-κB (31). Moreover, *p*12-LOX has also been reported to play a role in the reactive oxygen species generation in neuroblastoma cells (35). Accordingly, it is possible that the inhibition of *p*12-LOX suppresses neoplastic transformation of JB6 P+ cells which is caused, at least in part, by the decrease of TPA-induced reactive oxygen species generation.

These effects of the *p*12-LOX pathway on tumor promotion are similar to those of the COX-2/PGE_2 pathway in the gastrointestinal tumorigenesis. The activation of Wnt/β-catenin signaling causes the development of intestinal microadenoma (26). The subsequent induction of the COX-2/PGE_2 pathway in the microenvironment around the microadenoma is required for proliferation of small number of adenoma cells (3,36). Specifically, the inhibition of COX-2 or PGE_2 signaling suppresses proliferation of tumor cells in microadenoma (36,37). Importantly, these gastrointestinal tumors in mouse models also show the induction of the *p*12-LOX pathway as indicated in the present study. Therefore, it is possible that *p*12-LOX and COX-2 are two important pathways for tumor cell proliferation in the early stages. This is consistent with the findings of recent reports in which the polymorphism of either COX-2 or *p*12-LOX was shown to be associated with an increased risk of colon cancer development (38). Moreover, both COX-2 expression and 12(*S*)-HETE synthesis are induced in mouse prostate tumors (39). On the other hand, baicalein treatment failed to induce a regression of the established tumors in the immunodeficient mice. Accordingly, it is conceivable that the *p*12-LOX/12(*S*)-HETE pathway plays an important role particularly in the early promotion step like COX-2/PGE_2 pathway, rather than in the progression stage.

In conclusion, the present results demonstrated that *p*12-LOX is required for tumor promotion during epidermal cell transformation and 12(*S*)-HETE can accelerate tumorigenesis through enhancement of cloning efficiency. The expression of *p*12-LOX is induced also in the gastrointestinal tumors, suggesting that the *p*12-LOX pathway is an effective target for chemoprevention against skin carcinogenesis as well as gastrointestinal cancer.

Funding

Ministry of Education, Culture, Sports, Science and Technology of Japan, and Ministry of Health, Labor and Welfare of Japan.

Acknowledgements

We thank Manami Watanabe for valuable technical assistance.

Conflict of Interest Statement: None declared.

References

1. Shureiqi,I. *et al.* (2001) Lipoxygenase modulation to reverse carcinogenesis. *Cancer Res.*, **61**, 6307–6312.
2. DuBois,R.N. *et al.* (1998) Cyclooxygenase in biology and disease. *FASEB J.*, **12**, 1063–1073.
3. Oshima,M. *et al.* (1996) Suppression of intestinal polyposis in *Apc*$^{\Delta 716}$ knockout mice by inhibition of cyclooxygenase 2 (COX-2). *Cell*, **87**, 803–809.
4. Oshima,H. *et al.* (2004) Hyperplastic gastric tumors induced by activated macrophages in COX-2/mPGES-1 transgenic mice. *EMBO J.*, **23**, 1669–1678.
5. Oshima,H. *et al.* (2006) Carcinogenesis in mouse stomach by simultaneous activation of the Wnt signaling and prostaglandin E_2 pathway. *Gastroenterology*, **131**, 1086–1095.
6. Furstenberger,G. *et al.* (2006) What are cyclooxygenase and lipoxygenase doing in the driver's seat of carcinogenesis? *Int. J. Cancer*, **119**, 2247–2254.
7. Tang,K. *et al.* (1999) 12(*S*)-HETE in cancer metastasis. *Adv. Exp. Med. Biol.*, **447**, 181–191.
8. Yoshimoto,T. *et al.* (2002) Arachidonate 12-lipoxygenases. *Prostaglandins Other Lipid Mediat.*, **68–69**, 245–262.
9. Chen,Y.Q. *et al.* (1994) Endogenous 12(*S*)-HETE production by tumor cells and its role in metastasis. *Cancer Res.*, **54**, 1574–1579.
10. Gao,X. *et al.* (1995) Elevated 12-lipoxygenase mRNA expression correlates with advanced stage and poor differentiation of human prostate cancer. *Urology*, **46**, 227–237.
11. Timar,J. *et al.* (2000) Expression, subcellular localization and putative function of platelet-type 12-lipoxygenase in human prostate cancer cell line of different metastatic potential. *Int. J. Cancer*, **87**, 37–43.
12. Wong,B.C. *et al.* (2001) 12-Lipoxygenase inhibition induced apoptosis in human gastric cancer cells. *Carcinogenesis*, **22**, 1349–1354.
13. Raso,E. *et al.* (2004) Molecular identification, localization and function of platelet-type 12-lipoxygenase in human melanoma progression, under experimental and clinical conditions. *Melanoma Res.*, **14**, 245–250.
14. Krieg,P. *et al.* (1995) 12-Lipoxygenase isoenzymes in mouse skin tumor development. *Mol. Carcinog.*, **14**, 118–129.
15. Tong,W.G. *et al.* (2002) Lipoxygenase inhibitors attenuate growth of human pancreatic cancer xenografts and induce apoptosis through the mitochondrial pathway. *Mol. Cancer Ther.*, **1**, 929–935.
16. Tong,W.G. *et al.* (2002) The mechanisms of lipoxygenase inhibitor-induced apoptosis in human breast cancer cells. *Biochem. Biophys. Res. Commun.*, **296**, 942–948.
17. Leung,H.W.C. *et al.* (2007) Inhibition of 12-lipoxygenase during baicalein-induced human lung nonsmall carcinoma H460 cell apoptosis. *Food Chem. Toxicol.*, **45**, 403–411.
18. Ding,X.Z. *et al.* (2001) 12-Lipoxygenase metabolite 12(*S*)-HETE stimulates human pancreatic cancer cell proliferation via protein tyrosine phosphorylation and ERK activation. *Int. J. Cancer*, **94**, 630–636.
19. Pidgeon,G.P. *et al.* (2003) Overexpression of platelet-type 12-lipoxygenase promotes tumor cell survival by enhancing $\alpha_V\beta_3$ and $\alpha_V\beta_5$ integrin expression. *Cancer Res.*, **63**, 4258–4267.
20. Nie,D. *et al.* (2003) Increased metastatic potential in human prostate carcinoma cells by overexpression of arachidonate 12-lipoxygenase. *Clin. Exp. Metastasis*, **20**, 657–663.
21. Nie,D. *et al.* (2006) Mechanisms regulating tumor angiogenesis by 12-lipoxygenase in prostate cancer cells. *J. Biol. Chem.*, **281**, 18601–18609.
22. McCabe,N.P. *et al.* (2006) Vascular endothelial growth factor production in human prostate cancer cells is stimulated by overexpression of platelet 12-lipoxygenase. *Prostate*, **66**, 779–787.
23. Virmani,J. *et al.* (2001) Role of 'platelet-type' 12-lipoxygenase in skin carcinogenesis. *Cancer Lett.*, **162**, 161–165.
24. Colburn,N.H. *et al.* (1982) Phorbol diester and epidermal growth factor receptors in 12-*O*-tetradecanoylphorbol-13-acetate-resistant and -sensitive mouse epidermal cells. *Cancer Res.*, **42**, 3093–3097.
25. Bernstein,L.R. *et al.* (1989) AP1/jun function is differentially induced in promotion-sensitive and resistant JB6 cells. *Science*, **244**, 566–569.
26. Oshima,M. *et al.* (1995) Loss of *Apc* heterozygosity and abnormal tissue building in nascent intestinal polyps in mice carrying a truncated *Apc* gene. *Proc. Natl Acad. Sci. USA*, **92**, 4482–4486.
27. Miocinovic,R. *et al.* (2005) *In vivo* and *in vitro* effect of baicalein on human prostate cancer cells. *Int. J. Oncol.*, **26**, 241–246.
28. Deschamps,J.D. *et al.* (2006) Baicalein is a potent *in vitro* inhibitor against both reticulocyte 15-human and platelet 12-human lipoxygenase. *Bioorg. Med. Chem.*, **14**, 4295–4301.
29. Hsu,T.C. *et al.* (2001) Transformation non-responsive cells owe their resistance to lack of p65/NF-κB activation. *Cancer Res.*, **61**, 4160–4168.
30. Hu,J. *et al.* (2004) Insufficient p65 phosphorylation at S536 specifically contributes to the lack of NF-κB activation and transformation in resistant JB6 cells. *Carcinogenesis*, **25**, 1991–2003.
31. Dhar,A. *et al.* (2002) The role of AP-1, NF-κB and ROS/NOS in skin carcinogenesis: the JB6 model is predictive. *Mol. Cell. Biochem.*, **234/235**, 185–193.
32. Coussens,L.M. *et al.* (2002) Inflammation and cancer. *Nature*, **420**, 860–867.

33. Greten,F.R. *et al.* (2004) IKKβ links inflammation and tumorigenesis in a mouse model of colitis-associated cancer. *Cell*, **118**, 285–296.
34. Pikarsky,E. *et al.* (2004) NF-κB functions as a tumor promoter in inflammation-associated cancer. *Nature*, **431**, 461–466.
35. Lovat,P.E. *et al.* (2002) GADD153 and 12-lipoxygenase mediate fenretinide-induced apoptosis of neuroblastoma. *Cancer Res.*, **62**, 5158–5167.
36. Sonoshita,M. *et al.* (2001) Acceleration of intestinal polyposis through prostaglandin receptor EP2 in *Apc*^{1716} knockout mice. *Nat. Med.*, **7**, 1048–1051.
37. Oshima,M. *et al.* (2002) COX selectivity and animal models for colon cancer. *Curr. Pharm. Des.*, **8**, 1021–1034.
38. Tan,W. *et al.* (2007) Association of functional polymorphisms in *cyclooxygenase*-2 and platelet 12-lipoxygenase with risk of occurrence and advanced disease status of colorectal cancer. *Carcinogenesis*, **28**, 1197–1201.
39. Shappell,S.B. *et al.* (2003) Elevated expression of 12/15-lipoxygenase and cylclooxygenase-2 in a transgenic mouse model of prostate carcinoma. *Cancer Res.*, **63**, 2256–2267.

Received July 10, 2007; revised October 29, 2007; accepted November 24, 2007